A pilot-scale study of dynamic response scenarios for the flexible operation of post-combustion CO2 capture

International Journal of Greenhouse Gas Control xxx (2015) xxx–xxx

Contents lists available at ScienceDirect

International Journal of Greenhouse Gas Control

journal homepage: www.elsevier.com/locate/ijggc

A pilot-scale study of dynamic response scenarios for the flexible operation of post-combustion CO_2 capture

Paul Tait[a,*], Bill Buschle[a], Ilja Ausner[b], Prashant Valluri[a], Marc Wehrli[b], Mathieu Lucquiaud[a]

[a] University of Edinburgh, Institute for Materials and Processes, School of Engineering, Sanderson Building, The King's Buildings, Mayfield Road, Edinburgh EH9 3JL, United Kingdom
[b] Sulzer Chemtech Ltd, Sulzer-Allee 48, 8404 Winterthur, Switzerland

ARTICLE INFO

Article history:
Received 16 June 2015
Received in revised form
14 November 2015
Accepted 9 December 2015
Available online xxx

Keywords:
CO_2 capture
Post-combustion
NGCC
Flexibility
Dynamic operation
Pilot-plant

ABSTRACT

The ability to operate flexibly is critical for the future implementation of carbon capture and storage (CCS) in thermal power plants. A dynamic test campaign examines the response of a CO_2 absorption/desorption pilot-scale plant to realistic changes in flue gas flow rates and steam supply, representative of the operation of a Natural gas combined cycle (NGCC) plant fitted with post-combustion capture. Five scenarios, demonstrating the operational flexibility that is likely to be encountered in an energy market with significant penetration from intermittent renewables, are presented, with 30% monoethanolamine (MEA) as the absorbing solvent. It complements a wider effort on dynamic modelling of these systems where a lack of dynamic plant data has been reported.

The campaign focuses on analysing critical plant parameters of the response of the pilot plant to a gas turbine shutdown, a gas turbine startup and three enhanced operational flexibility scenarios, including two for power output maximisation and one for frequency response with a rapid increase of steam supply to the reboiler. The campaign also demonstrates the use of continuous in situ solvent lean loading measurement with the use of a novel online continuous liquid sensor.

It confirms that no significant barriers to flexible operation of amine post-combustion capture are found, although there remains scope for the improvement of plant response. Solvent inventory and circulation times are found to have a significant effect on capture rate during certain dynamic operations. A large solvent inventory increases total circulation times, which can result in additional time being required for the plant to return to steady state following a perturbation. The plant is forced to operate with a non-optimal capture rate while the solvent loading at the absorber inlet stabilises is identified as a potential impact.

Use of interim solvent storage and continuous online measurement of solvent CO_2 loading, combined with comprehensive knowledge of liquid circulation times and potential mixing effects, are suggested as methods for improving plant response to dynamic operation, thereby increasing CCS plant flexibility.

1. Introduction

In any energy generation portfolio with considerable input from renewable sources such as wind and solar, natural gas or coal-fired thermal power stations will be required to meet variable demand during periods when these intermittent sources are not generating electricity (Pöyry, 2009). As investment in low-carbon renewable technologies continues, the dispatch patterns of thermal power stations will become less regular, with rapid ramping, startup and shutdown operations based on changing weather patterns becoming commonplace (Murray, 2013).

If carbon emission targets are to be met at an acceptable cost to society, thermal power stations must be fitted with carbon capture and storage (CCS) technology. For example, an analysis of possible power sector decarbonisation scenarios for the UK predicts that without CCS, the cost of delivering climate change targets will double from 1% to 2% of GDP (ETI, 2015). The latest IPCC report (IPCC, 2014) states that in 6/10 predicted scenarios, it is not possible to

* Corresponding author.
E-mail address: p.tait@ed.ac.uk (P. Tait).

http://dx.doi.org/10.1016/j.ijggc.2015.12.009

Index of terms

α	solvent loading (mol CO_2/mol alkalinity)
N	molar flow rate (mol/s)
η	CO_2 capture rate (fractional)

mitigate climate change to within +2 °C with no deployment of CCS and shows significant increase in the costs of mitigation if the technology is not available.

Of the available technologies for CCS in power generation, post-combustion capture (PCC) with amines is a mature and established technology, with an operational full-scale facility on 120 MW coal fired plant at Boundary Dam, Canada, a planned 385 MW project on a natural gas-fired plant at Peterhead, Scotland and numerous pilot-scale facilities worldwide (GCCSI, 2014). However, the majority of research carried out on PCC at the time of writing has assumed steady-state operation with a consistent power plant output and flue gas flow rate/composition. When predicted plant dispatch patterns for electricity generation scenarios which include significant penetration from intermittent renewable sources are considered, it is increasingly likely that dynamic and flexible operation will be highly relevant.

There is a large body of work on the dynamic modelling of PCC; however, there remains a lack of dynamic plant data, leading to many studies being unvalidated or validated using steady-state data, as discussed in an extensive review by Bui et al. (2014). Faber et al. (2011) and Bui et al. (2013) have proposed implementing a series of step-changes in order to obtain dynamic data for model validation. This method has been used successfully to validate the dynamic simulation of PCC for coal (Flø et al., 2014) and NGCC (Flø et al., 2015) flue gas. While step-changes in a single plant variable are useful for the purposes of validation, they are unlikely to be representative of how a real PCC plant will operate under transient conditions. Additionally, a model validated with data from one pilot facility may not agree with one which is validated with data obtained from another, as differences in plant design, liquid inventory and solvent properties can significantly affect dynamic operation (Kvamsdal et al., 2011).

Several modelling studies which investigate realistic scenarios and enhanced plant flexibility are present in the literature. Haines and Davison (2014) have shown the effect of adding flexibility via a rapid "stripper stop" operation, providing a rapid boost of power to the grid by decreasing the flow of steam extracted from the IP/LP crossover. Mac Dowell and Shah (2014) analyse several strategies which could increase profitability for coal plant operators via flexible PCC operation. Ceccarelli et al. (2014) provide an in-depth analysis of load-following, startup and shutdown operations for a PCC retrofit on CCGT plant, with a focus on reducing CO_2 emissions. However, none of these studies are validated with dynamic plant data.

Pilot-scale test campaigns on realistic dynamic operating scenarios are necessary to obtain more data for model validation and provide a more complete understanding of how CCS plants respond to variations in generation plant output. This knowledge allows researchers to devise operating strategies and develop hardware and software capabilities to increase flexibility, allowing PCC to cope with rapidly-changing generation plant output.

In this test campaign the response of a CO_2 absorption/desorption pilot-scale plant to five dynamic operating scenarios is examined. Changes in the flow rate of solvent, flue gas and steam supply are designed to be proportional to, and representative of the operation of a natural gas combined cycle (NGCC) plant fitted with PCC. The focus is on NGCC plants since they offer favourable dynamic operating capability, with short times for startup, ramping

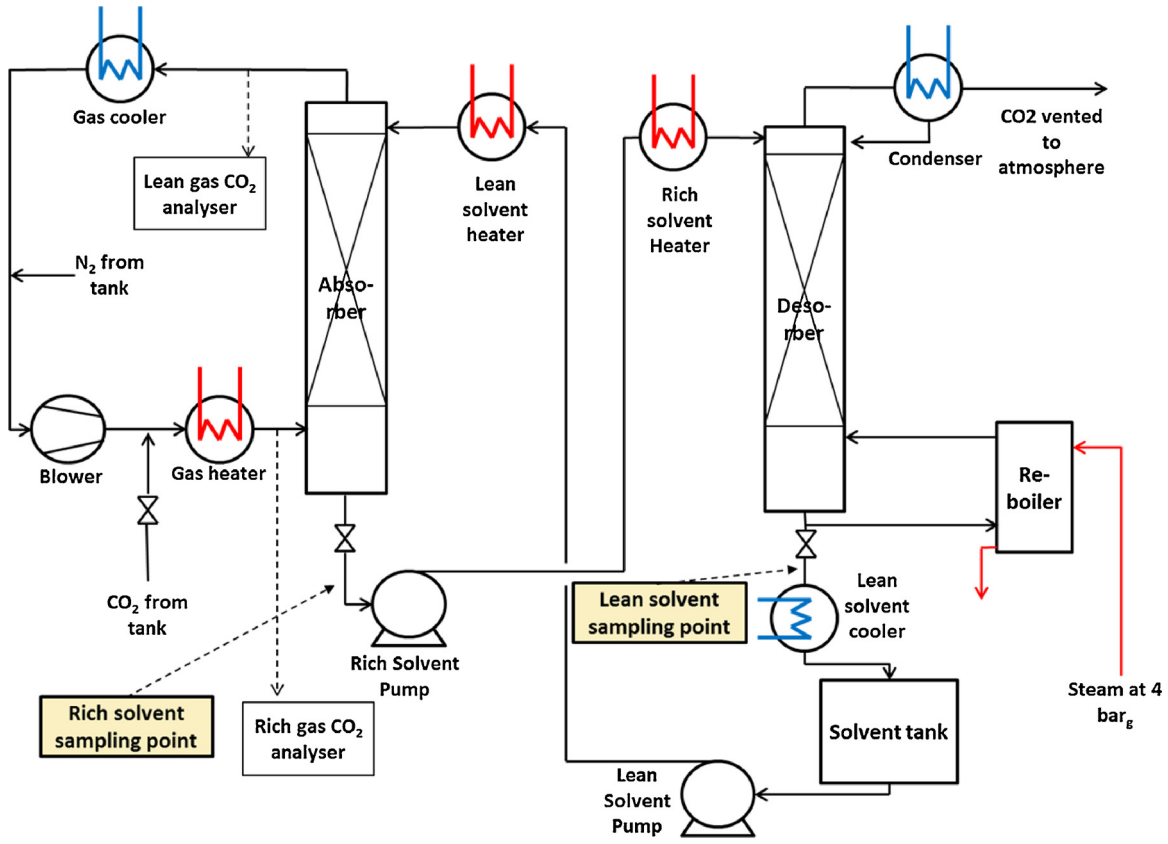

Fig. 1. Absorption/desorption test facility process flow diagram.

Please cite this article in press as: Tait, P., et al., A pilot-scale study of dynamic response scenarios for the flexible operation of post-combustion CO_2 capture. Int. J. Greenhouse Gas Control (2015), http://dx.doi.org/10.1016/j.ijggc.2015.12.009

Table 1
Comparison of pilot-scale test facilities (Seibert et al., 2011; Kvamsdal et al., 2011; Notz et al., 2012; Rabensteiner et al., 2014).

Pilot facility	Absorber inner diameter (mm)	Height of packed bed (m)	Packing type	Has cross-heat exchanger Y/N
University of Texas at Austin, Separations Research Program	427	3.07 × 2	Raschig Super-Pak 250	Y
NTNU/SINTEF, VOCC (Validation Of Carbon Capture)	500	5.4	Sulzer Mellapak 2X	Y
University of Stuttgart	125	4.2	Sulzer Mellapak 250.Y	Y
Graz University of Technology, Dürnrohr power station	150	12	Raschig Super-Pak 250	Y
Sulzer Chemtech absorption/desorption test facility, this work	158	6.92	Sulzer Mellapak 250.X	N

and load response, and are likely to play a significant role in providing dispatchable electricity infills for intermittency management in future energy generation mixes. Although current carbon budgets suggest that gas CCS will be important (ETI, 2015) and that a gradual phase-out of coal generation is necessary between now and 2030 in order to meet emissions targets (CCC, 2013), the outcomes could also be applicable to PCC on coal, which is a very similar process to PCC on gas but with less stringent ramping requirements and higher CO_2 concentration in the flue gas.

The pilot-scale facilities of Sulzer Chemtech in Winterthur, Switzerland are configured for atmospheric pressure post-combustion capture and are complemented, in some of the dynamic scenarios, by continuous in situ solvent lean loading measurement with the use of a novel online continuous liquid sensor. An overview of the test facility, measurement techniques and metrics is provided, five relevant dynamic operating scenarios are presented, and the results of the implementation of each scenario during the test campaign are discussed. Full dynamic data obtained from these scenarios are supplied as an attachment to the electronic version of this paper.

2. Carbon dioxide absorption/desorption test facility

2.1. Plant description

The pilot plant used in this study, represented schematically in Fig. 1, is controlled and monitored using a combination of Labview software and discrete panel-mounted PID microcontrollers. Synthetic flue gas, composed of N_2 and CO_2, is used. Nitrogen is fed to the facility from a tank upstream of a gas blower. After the blower, a mass flow controller determines the rate at which CO_2 is fed to the gas line. For this test campaign, an inlet CO_2 concentration representative of NGCC exhaust (4.3%, v/v) is achieved with a cascade PID control system of the CO2 mass flow controller. The flue gas is heated to an inlet temperature of approx. 45 °C, before entering the absorber column. After exiting the absorber, flue gas is analysed for CO_2 content in order to determine the capture rate, before being cooled and recycled by feeding back to the blower. While not truly representative of real PCC plant operation, this reduces nitrogen usage, and ensures that the majority of the gas stream becomes rapidly saturated, reducing water losses via evaporation in the absorber.

The solvent tank can hold up to 500 l, and 116.8 kg neat monoethanolamine (MEA) and 270.5 kg deionised H_2O were introduced to produce a solution of 30.16% (w/w) MEA. During plant operation, with solvent circulating in the pipework and vessels, the solvent tank inventory generally remained at around 10% of its maximum level. At the flow rates used in this experimental work, between 40 min and 113 min is required for the entire solvent inventory to circulate once through the plant. The associated effect on plant response is discussed in detail later in this paper.

The main solvent pump circulates liquid to the top of the absorber, where it is heated to approx. 40 °C. The intent is to reproduce the effect of a cross-flow solvent heat exchanger. The absorber sump level is maintained using a Varibell control valve. Upon exiting the absorber, a secondary pump circulates the liquid to the top of the desorber, which is held at a pressure of approx. 1.8 bar.

Steam at a pressure of 5 bar (absolute) is used for solvent regeneration and other heating, for example, mimicking the effect of a cross-flow heat exchanger. CO_2 and water vapour exit the top of the desorber, where the water is condensed and CO_2 vented to atmosphere.

The concentrations of CO_2 at the absorber inlet and outlet are monitored using infra-red (IR) CO_2 analysers. Lean and rich solvent loading are determined by manual sampling at the desorber and absorber outlet, followed by benchtop titration analysis. At standard operating conditions (Table 2) solvent takes approx. 40 min to circulate through the plant, leading to time delays between e.g. a lean sample being taken and this discrete "packet" of solvent reaching the absorber inlet. This effect is exacerbated further at lower flow rates and must be taken into consideration when relating variations in loading to those in capture rate.

The absorber has an inner diameter of 158 mm and contained 6.92 m of Sulzer Mellapak 250.X packing. The desorber has an inner diameter of 350 mm and contained 5.00 m of Sulzer Mellapak 500.X packing. Absorber dimensions are comparable to other pilot plants, as illustrated in Table 1.

The facility in this work is used for a range of applications and is not designed specifically for post-combustion capture at atmospheric pressure. Unlike other pilot plants reported in Table 1, which utilise a cross-heat exchanger to increase the temperature of the rich solvent, the pilot plant used in this study does not have this capability so the effect is simulated using separate heat exchangers. Using a setpoint of 20 °C below the outlet temperature, a rich solvent heater increases the liquid temperature at the desorber inlet. The solvent is cooled to room temperature before entering the main solvent tank, then heated to approx. 40 °C before entering the absorber. A PID control loop with steam supply is used to control the solvent temperature at absorber and desorber inlets. Temperature settings are selected to be representative of the typical temperature pinch of a cross flow heat exchanger (Table 2).

3. Test campaign methodology and preparation

3.1. Determination of baseload operating conditions

The purpose of the test campaign is to implement dynamic post-combustion capture scenarios using a test facility configuration which approximates a PCC pilot plant. A reference "baseload"

Please cite this article in press as: Tait, P., et al., A pilot-scale study of dynamic response scenarios for the flexible operation of post-combustion CO_2 capture. Int. J. Greenhouse Gas Control (2015), http://dx.doi.org/10.1016/j.ijggc.2015.12.009

Table 2
Summary of baseload operating conditions.

Controlled variable	Value
Gas flow rate at absorber inlet (N m^3/h)	120.5
Gas inlet temperature (°C)	46.14
Inlet gas CO_2 concentration (%, v/v)	4.27
Steam flow rate (kg/h)	19.5
Liquid flow rate (l/h)	344.4
Steam pressure (bar_a)	4.0
Desorber pressure (bar_a)	1.80
Liquid inlet temperature, absorber (°C)	40.05
Liquid inlet temperature, desorber (°C)	104.07
Measured parameter	**Value**
CO_2 capture rate (%)	89.7
Reboiler duty (GJ/tCO_2)	3.96
L/*G* ratio (l/m^3)	2.86
Lean solvent loading (mol amine/mol CO_2)	0.232
Rich solvent loading (mol amine/mol CO_2)	0.345

operation scenario, which all other scenarios are carried out in comparison to, is first determined.

Thirty percent (w/w) MEA solution is used as a liquid absorbent, since it is commonly used as a benchmark for pilot-scale facilities worldwide (Fitzgerald et al., 2014; Hamborg et al., 2014; Artanto et al., 2012).

A desired baseload capture rate of 90% is selected in order to remain consistent with other pilot-scale studies (Rabensteiner et al., 2014; Carey et al., 2013; Mejdell et al., 2011).

Previous work on natural gas flue gas capture (Ystad et al., 2012) indicates that for 30% (w/w) MEA, the liquid to gas flow ratio (*L*/*G*) which results in the lowest energy expenditure per ton CO_2 captured is approx. 1.5l solvent per m^3 gas. Flue gas flow rate is kept constant at 115 m^3/h. With further addition of CO_2 at a rate of approx. 8.1 kg/h and an inlet CO_2 concentration of 4.3% (v/v) (moist), an *f*-factor of 1.85 $Pa^{0.5}$ is obtained. Liquid flow rate is varied to obtain *L*/*G* ratios between 2.4 and 3.6 l/N m^3. For each ratio, at a desorber pressure of 0.8 bar_g, the flow rate of steam to the reboiler at 4 bar_g is increased until a CO_2 capture rate of 90% is achieved. A minimum reboiler duty of 3.96 GJ/tCO_2 for this plant is observed at an *L*/*G* ratio of 2.858 l/m^3. Typical reboiler duty values for NGCC base case studies have been reported between 3.4 and 4.04 GJ/tCO_2 (Jordal et al., 2012).

It should be noted that the lean loading is low in comparison to what would be expected in a capture plant which is purpose-built and optimised for NGCC flue gas, due to a lack of packing height in the absorber compared to current modelling studies (Biliyok et al., 2014; Rabensteiner et al., 2014). In order to compensate and achieve 90% capture, a lower lean loading is used to enhance the driving force for CO_2 absorption and the liquid flow rate is increased. This results in a similarly low rich loading, with the effect being exacerbated as the increased liquid flow rate results in a smaller difference in loading between the liquid inlet and outlet. An alternative strategy would be to accept a lower CO_2 capture rate while maintaining more representative values of *L*/*G* ratio, lean loading and rich loading, but due to equipment limitations caused by the turndown ratio of the liquid pump and steam inlet valve, further reductions in flow rate would result in considerable flow instability, especially during dynamic scenarios which require additional turndown. Increasing the gas flow rate is also not an option, as the blower has a maximum flow rate of around 130 N m^3/h due to the pressure drop of the packing and liquid holdup.

Additionally, the energy input to the absorber and desorber solvent trim heaters is not accounted for, due to the absence of steam flow rate measurement to each heat exchanger. It is possible that the reboiler inlet liquid temperature is unrealistically high, so less energy is required to provide sensible heat, and if a cross-heat exchanger were installed a higher reboiler duty would be observed. This seems likely, as the figure of 3.96 GJ/tCO_2 is still within the reported range of typical values, with a liquid flow rate which is much higher than optimal.

A full list of conditions is summarised in Table 2.

To allow for comparison with real plant ramping events and future pilot plant campaigns, all flow rates and ramp rates in the dynamic scenarios investigated are subsequently referred to as percentages of this baseload condition.

Due to the low loadings, the solvent retains unused capacity of approximately 0.155 mol CO_2/mol free amine at the bottom of the absorber. This results in a significant driving force in this location during baseload operation. During dynamic scenarios which involve shutdown or reduction of stripping steam, this additional capacity will allow the plant to continue to capture CO_2 for longer periods of time than if the plant were operated with a rich loading which is closer to equilibrium with the inlet gas CO_2 concentration.

3.2. Plant lag times

The mass inertia of the solvent inventory has an effect on the dynamic response of the plant. Solvent circulation time is obviously dependent on total solvent inventory, which is limited in this study to as little as practically possible. Circulation times at several different liquid flow rates are estimated by inducing a step-change in main pump output, and observing the time required for this to produce a liquid level change of 10% at several points in the liquid line. The solvent pump reaches its new setpoint within approx. 10 s and does not contribute significantly to the overall circulation time. The results are summarised in Table 3. Circulation times between each individual section of the plant, and relevant circulation times at 50% of solvent baseload flow rate are estimated using the measured values and indicated by *. Circulation times through sumps are estimated using (circulation time = liquid holdup/volumetric flow rate) (Fig. 2).

Solvent circulation times have a direct impact on the dynamic response of the capture plant and affect the time delay between when a process parameter is changed and when the impact of that change is observed in solvent loading and plant capture rate. For example, after a change in steam flow rate to the reboiler, it takes approximately 30 min (Table 3) at 100% baseload flow rate for the change in lean solvent loading to be observed at the rich solvent sampling point based on solvent circulation times. The amount of solvent in the vessel sumps and solvent tank, and solvent mixing also has an impact on the dynamic response of the plant (Table 4).

3.3. Rationales for the choice of dynamic scenarios

Five dynamic scenarios are carried out, with the intent of representing to real plant operation as much as practically possible. They are separated into two categories:

Shutdown and startup scenarios

1. Gas turbine shutdown

The shutdown sequence represents a realistic scenario based on the shutdown sequence of a modern NGCC plant. The gas turbine ramp rates in this and the gas turbine startup scenario are characteristic of a SIEMENS STG5-4000F (Eisfeld and Feldmüller, 2013), and are detailed in Sections 5.1 and 5.2 respectively. The method by which the plant is shut down directly impacts its performance upon restart. Ceccarelli et al. (2014) model two generation/capture plant shutdown cases, one of which is implemented in this work. Liquid and gas flow rates are ramped down simultaneously, maintaining a constant *L*/*G* flow ratio over the course of the shutdown operation until both reach 30% of

Please cite this article in press as: Tait, P., et al., A pilot-scale study of dynamic response scenarios for the flexible operation of post-combustion CO_2 capture. Int. J. Greenhouse Gas Control (2015), http://dx.doi.org/10.1016/j.ijggc.2015.12.009

Table 3
Summary of plant solvent circulation times.

Liquid flow rate (as percentage of baseload)	Circulation time from main solvent pump to top of absorber sump (min:sec)	Circulation time from top of absorber sump to top of desorber sump (min:sec)	Circulation time from top of desorber sump to top of 500 l liquid tank (min:sec)	Circulation time from top of liquid tank to main solvent pump (min:sec)	Total circulation time required (min:sec)	Circulation time from lean sample point to rich sample point* (min:sec)
100	1:07	6:03	8:35	21:10	36:55	30:17*
75	1:20	7:25	10:36	32:17	51:38	43:38*
50*	1:49*	8:40*	14:25*	48:58*	73:52*	63:11*
30	2:20	12:18	19:40	79:35	113:08	97:50*

* Estimated values based on other measurements.

Table 4
Estimated circulation times (in min:sec) between relevant plant locations.

	100% of baseload	75% of baseload	50% of baseload	30% of baseload
Main solvent pump – absorber inlet	0:20*	0:27*	0:40*	0:55*
Absorber inlet – top of absorber sump	0:47*	0:53*	1:09*	1:25*
Top of absorber sump – rich sampling port (absorber sump outlet)	2:10*	2:55*	3:24*	5:08*
Rich sampling port (absorber sump outlet) – desorber inlet	3:06*	3:37*	4:07*	5:45*
Desorber inlet – top of desorber sump	0:47*	0:53*	1:09*	1:25*
Top of desorber sump – lean sampling port (desorber sump outlet)	2:45*	3:30*	5:25*	9:03*
Lean sampling port (desorber sump outlet) – top of 500l solvent tank	5:50*	7:06*	9:00*	10:37*
Top of 500 l solvent tank – main solvent pump	21:10*	32:17*	48:58*	79:35*
Total circulation time	36:55	51:38	73:52*	113:53

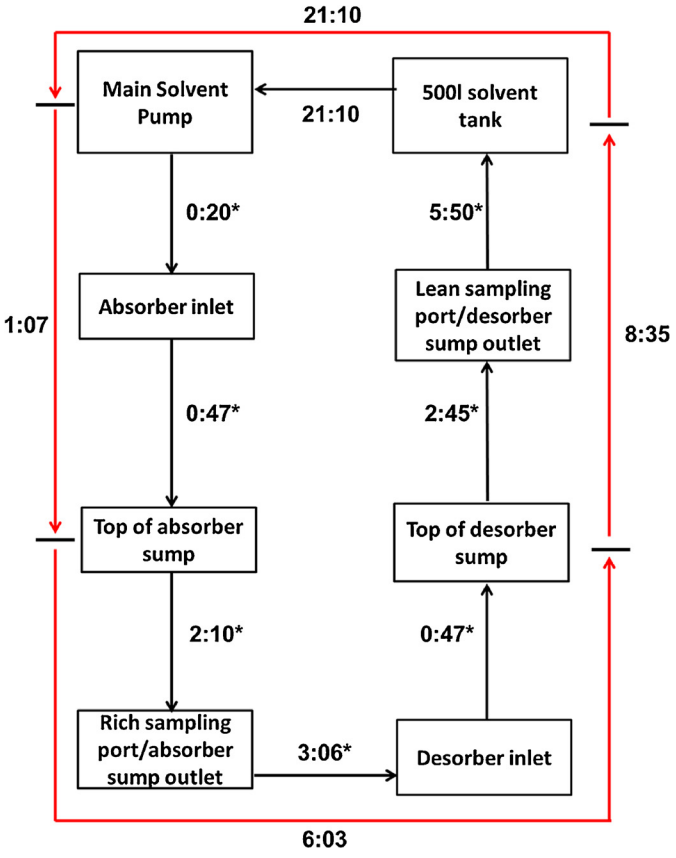

Fig. 2. Block diagram of plant solvent circulation times (in min:sec) for baseload solvent flow rate. * indicates estimated value based on other measurements.

baseload. Gas flow continues to ramp down to zero, while liquid flow is maintained at 30% to make use of the plant's cooling duty, resulting in a cooler solvent and promoting CO_2 absorption upon startup. There is, however, some trade-off in implementing this strategy, as the continued circulation causes lean and rich solvent loadings to converge due to mixing effects. This may affect CO_2 absorption performance when the plant is restarted.

2. Gas turbine startup

Plant startup is simulated to follow a shutdown event in which the flow of solvent has been maintained at 30% of baseload, causing solvent temperature to be reduced to <35 °C, and lean and rich loading to begin to converge due to mixing. Before the startup sequence is initiated, liquid flow rate is stabilised at 30% of baseload flow rate. Ramp rates for the startup operation are based on an NGCC plant using a state-of-the-art SIEMENS STG5-4000F gas turbine (Eisfeld and Feldmüller, 2013), as with the gas-turbine shutdown scenario, and are provided in Section 5.2. Liquid flow rate is ramped proportionally to that of the gas, maintaining a constant *L*/*G* flow ratio.

Enhanced operational flexibility scenarios

1. Power output maximisation by capture plant decoupling

The flow of steam to the reboiler and the flow of flue gas entering the absorber column are rapidly stopped. This represents a by-pass of the capture plant, where steam for solvent regeneration is redirected to the combined cycle, the CO_2 compressors are shut down and the flue gas is vented directly to atmosphere after the heat recovery steam generator (HRSG). Solvent flow rate is reduced to 50% to reduce the power consumption of the pumps and the extent to which the lean and rich solvent loading will average, due to mixing effects. This mode of operation increases flow rate of steam to the low-pressure (LP) turbine and hence power plant electricity output. It is a useful capability during instances when the selling price of electricity is high, rapidly increasing the amount of energy available for dispatch to the grid (Haines and Davison, 2014). It should be noted that the viability of this scenario depends on carbon cost, electricity selling price and specific regulations regarding emissions costs. Flue gas venting is uneconomical when CO_2 prices are high in comparison to the selling price of electricity.

2. Power output maximisation by reboiler steam decoupling only

This scenario rapidly stops the flow of steam to the reboiler, while flue gas continues to flow through the absorber. This method of operation is similar to capture plant decoupling, but could also be utilised in power plants, where the ability to bypass the absorber has not been implemented or if some level of

Please cite this article in press as: Tait, P., et al., A pilot-scale study of dynamic response scenarios for the flexible operation of post-combustion CO_2 capture. Int. J. Greenhouse Gas Control (2015), http://dx.doi.org/10.1016/j.ijggc.2015.12.009

capture is still desirable. Again, solvent flow rate is reduced to 50% for the reasons stated above.

3. Frequency response increase by rapid reboiler steam flow increase

In this operation, the flow of steam to the reboiler is rapidly increased to reach 200% of the baseload value. It could be used in power plants as a complementary method of rapidly decreasing plant electricity output where steam extraction from the combined cycle is ramped up as much as practically possible, in response to a requirement to maintain grid frequency within acceptable limits. A doubling of steam extraction from the combined cycle of a gas power plant is consistent with maintaining a minimum steam flow rate at the inlet of the low pressure turbine for blade cooling. With the increase in steam flow rate there exists a risk of accelerating solvent thermal degradation due to the creation of "hot spots" on the heat exchanger, but this will be plant/solvent specific and could be mitigated via plant design or solvent control methods.

For all data presented, the dynamic scenario is initiated at $t = 0$ min. To illustrate that the plant is initially operating at steady state, data was logged for a period of several minutes prior to the first dynamic perturbation. Everything before $t = 0$ is referred to in terms of negative values of time. However, upon analysing the data after the completion of the test campaign, it appears that steady-state operation is not always achieved.

3.4. Solvent circulation times and estimation of real-time solvent working capacity

To effectively understand the impact of dynamic scenarios on solvent CO_2 loading at the absorber inlet and outlet, time-shifting is utilised in order to estimate the time at which each "packet" of lean or rich solvent taken for analysis will reach the absorber packed bed inlet or outlet, respectively. The continuous online solvent measurement is also time-shifted using the same method. This is illustrated in Figs. 8c, 10c, 12c and 14c. It is possible to estimate when each discrete packet of solvent sampled at the lean inlet reaches the absorber, by estimating the total solvent inventory between the lean sampling port and the absorber inlet and dividing by the flow rate. It is also possible to determine when each rich solvent sample reaches the base of the packed bed by estimating the time required to flow through the absorber sump. The forward time-shifting of the lean loading measurements does not account for potential mixing effects in the main solvent tank, nor does the backwards time-shifting of rich loading measurements account for mixing effects in the absorber sump, as both rely on the assumption of plug flow. This time-shifting method has been applied to lean and rich titration measurements and continuous lean loading measurement values in Figs. 8c, 10c, 12c and 14c, in order to more effectively illustrate how the CO_2 capture rate responds to changes in solvent lean loading. The driving force for CO_2 absorption by the working solvent is dependent on its inlet CO_2 loading, and shifting the lean loading measurements to the absorber inlet shows more clearly how the capture rate and lean loading are related. However, the time-shifting method is unable to account for potential mixing effects in the solvent tank and pipework.

Since the times that the rich and lean samples taken for bench measurements generally do not match, the real-time solvent working capacity (defined as the difference in solvent loading between the absorber inlet and absorber outlet at any given point in time) is estimated using the capture rate and flow rates of CO_2 and MEA. This can be done using two methods:

1. Each lean loading bench measurement is time-shifted forward to the time where it enters the absorber inlet, rich loading at the base of the packing is then estimated using the average capture rate and flow rates of CO_2 and MEA over the following minute

$$\alpha_{\text{rich,calculated}} = \alpha_{\text{lean,measured}} + \left(\frac{\dot{N}_{CO_2} \times \eta_{CO_2}}{\dot{N}_{MEA}} \right)$$

2. Each rich loading bench measurement is time-shifted backwards to the time where it reaches the base of the absorber packing, lean loading at the absorber inlet is then estimated using the average capture rates and flow rates of CO_2 and MEA over the previous minute.

$$\alpha_{\text{lean,calculated}} = \alpha_{\text{rich,measured}} - \left(\frac{\dot{N}_{CO_2} \times \eta_{CO_2}}{\dot{N}_{MEA}} \right)$$

3.5. Uncertainty analysis of titration measurements

Based on the analysis of 14 triplicate measurement sets, 42 measurements in total, the expanded repeatability ($k = 2$) is estimated to be ±4.54% of the measured value. The accuracy estimate is ±0.63% of the measured value, based on a single measurement of a 1.110 wt% CO_2 standard. Therefore, the expanded uncertainty estimation for the method is ±5.2% relative (rounded to 2 significant figures) with a coverage factor of $k = 2$. A Bland–Altman plot shows that 40 of 42 measurements have a relative deviation from the mean value which is within 5.2% or lower, and thus the confidence level is approximately 95%. In future test campaigns the uncertainty analysis should be improved, utilising multiple measurements of CO_2 standards which have a range of different CO_2 concentrations. Additionally, it is assumed that the nominal amine concentration remains constant throughout the test campaign, when in reality it may vary due to water losses and/or solvent degradation.

3.6. Relationship between absorber temperature bulge and real-time solvent working capacity

Calculated real-time solvent capacity measurements are plotted against the temperature at the hottest part of the absorber during baseload operation, at 4.65 m of packing height (Fig. 3).

The majority of the solvent loading capacity data points fall within 20% of the value predicted by the correlation. It should be noted that solvent capacity values are calculated using the time-shifting estimation discussed in Section 3.4, and mixing effects could have resulted in errors in the calculation. The solvent working capacity may also respond faster to changes in plant operation than the temperature bulge, due to the thermal inertia of the absorber column. This results in a poor correlation, and as such the temperature bulge is not thought to be an effective indicator of solvent working capacity during transient operations.

4. Online solvent loading sensor

A novel liquid sensor which differs from previous online measurement techniques (e.g. van Eckeveld et al., 2014) has been developed in-house at Edinburgh University. The sensor is used for continuous measurement of solvent lean loading in three of the dynamic scenarios.

It uses in situ measurements of physical properties to determine solvent loading and amine concentration, using proprietary intellectual property which is under development at the time of writing. Knowledge of the solvent CO_2 loading in real-time can provide CCS plant operators with more frequent solvent analysis measurements, enabling them to react rapidly to perturbations or disturbances and develop automated process control systems

Please cite this article in press as: Tait, P., et al., A pilot-scale study of dynamic response scenarios for the flexible operation of post-combustion CO_2 capture. Int. J. Greenhouse Gas Control (2015), http://dx.doi.org/10.1016/j.ijggc.2015.12.009

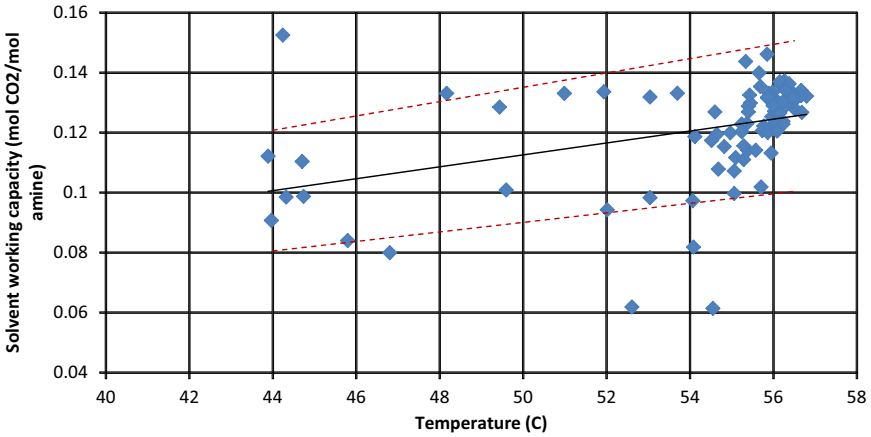

Fig. 3. Correlation between calculated solvent working capacity and temperature at packing height of 4.65 m, all scenarios.

for dynamic plant operation. Anecdotal evidence suggests that the established state-of the art for determination of solvent CO_2 loading is accomplished via the use of an online auto-titrator which can take around 20 min or longer. As demonstrated in this work, plant conditions can change significantly within this period of time, therefore a more rapid method of solvent loading determination must be developed in order to incorporate solvent physical properties into future plant control systems.

The online sensor provides a continuous measurement of solvent loading and amine concentration. Further discussion of the operating principle is not possible as the technology is considered commercially sensitive.

Two locations are tested in this study, as illustrated in Figs. 4 and 5, where the online solvent lean loading sensor takes a slipstream of liquid from the lean solvent line.

For the "gas turbine startup" and "power output maximisation by capture plant decoupling" scenario, the sensor is located in the lean solvent line upstream of the solvent tank, between the desorber sump outlet and the main solvent tank. For the scenarios "power output maximisation by reboiler steam decoupling" and "frequency response" it is located downstream of the solvent tank and the main solvent pump. The sensor output is time-shifted to the point at which each "packet" of lean solvent analysed exits the desorber sump, for comparison with titration measurements. The sensor was unavailable for the "gas-turbine shutdown scenario".

5. Dynamic scenarios – results and discussion

5.1. Gas turbine shutdown

The shutdown sequence is initiated at $t = 0$ min as shown in Fig. 6a. Steam flow rate is ramped down to zero over 10 min at a rate of 10% of baseload/min, as is representative of state-of the-art gas turbine operation. Liquid and gas flow rates are ramped down simultaneously at a rate of 2.5%/min for a period of 16 min. At $t = 16$ min, the shutdown rate of liquid and gas was changed to 7.5% of baseload/min. At $t = 20$ min, liquid and gas flow rates both reach 30% of baseload. The liquid flow rate is held at this value, while the gas flow is further reduced at a rate of 15%/min until it reaches zero. Gas flow rate reaches zero at $t = 22$ min, while liquid flow is maintained at 30% of baseload until the absorber temperature bulge has subsided (Fig. 7).

The solvent lean loading at the desorber outlet begins to rise sometime between $t = 5$ min and $t = 10$ min due to the reduction in steam flow to the reboiler. Assuming plug flow and no mixing in the solvent tank, the more CO_2-rich "packet" of solvent sampled at $t = 10$ min does not reach the absorber inlet before the gas flow rate reaches zero, using the estimated solvent circulation times as described in Section 3.4. Lean loading at the desorber outlet increases throughout the shutdown operation, but has no significant effect on capture rate as this "richer" lean solvent is not predicted to reach the absorber inlet before of the flow rate of gas reaches zero.

Capture rate is observed to increase from 90% to 97.5% as gas and liquid flow is reduced (Fig. 6b). Since the solvent flow rate is gradually ramped down, the liquid holdup in the absorber requires additional time (compared to baseload) to flow over the packing and into the absorber sump. Although the L/G flow ratio is controlled to remain constant, the flow rate of gas passing through the absorber decreases more rapidly than the liquid holdup on the packing it comes into contact with, so a greater proportion of the CO_2 in the flue gas may be absorbed as the gas flow rate approaches and eventually drops to zero. Furthermore, the increased residence time of liquid and gas in the absorber column could result in this increased capture rate.

Although capture rate increases, the temperature profile of the absorber (Fig. 7) decreases in magnitude, as the absolute rate of exothermic CO_2 absorption decreases as the gas flow rate approaches zero. After the flow of gas is stopped at $t = 20$ min, the location of the temperature bulge decreases in magnitude and moves down the packing height. Fig. 7 illustrates the evolution of the absorber temperature profile as hot solvent flows down the packed bed and into the absorber sump, with the packing hold up being replaced by slow flowing, semi-stagnant cooler solvent.

Although no exothermic absorption reaction is taking place, residual heat in the metal elements of the absorber column combined with additional insulation to prevent heat loss, result in the absorber requiring some time to cool down.

It should be noted that the values of temperature at a height of 7.1 m in Fig. 7, and all other figures which represent the temperature profile, refer to a temperature measured directly before the absorber inlet. Heat transfer between the gas flow rate and solvent inventory in liquid distributors can, in practice, be neglected to a first order approximation.

It is important to note that the rich and lean loading values, shown in Fig. 6b, are not representative of the solvent loading at the absorber inlet and outlet at the reported time, and instead represent the loadings at the outlet of the desorber (lean) and absorber (rich) sumps, from where solvent samples were manually taken. In other dynamic scenarios with a longer duration, it is possible to estimate the circulation time required for a "packet" of solvent to reach the absorber inlet and outlet from each sampling port and hence, the real-time solvent working capacity, as explained previously in Section 3.4.

Please cite this article in press as: Tait, P., et al., A pilot-scale study of dynamic response scenarios for the flexible operation of post-combustion CO_2 capture. Int. J. Greenhouse Gas Control (2015), http://dx.doi.org/10.1016/j.ijggc.2015.12.009

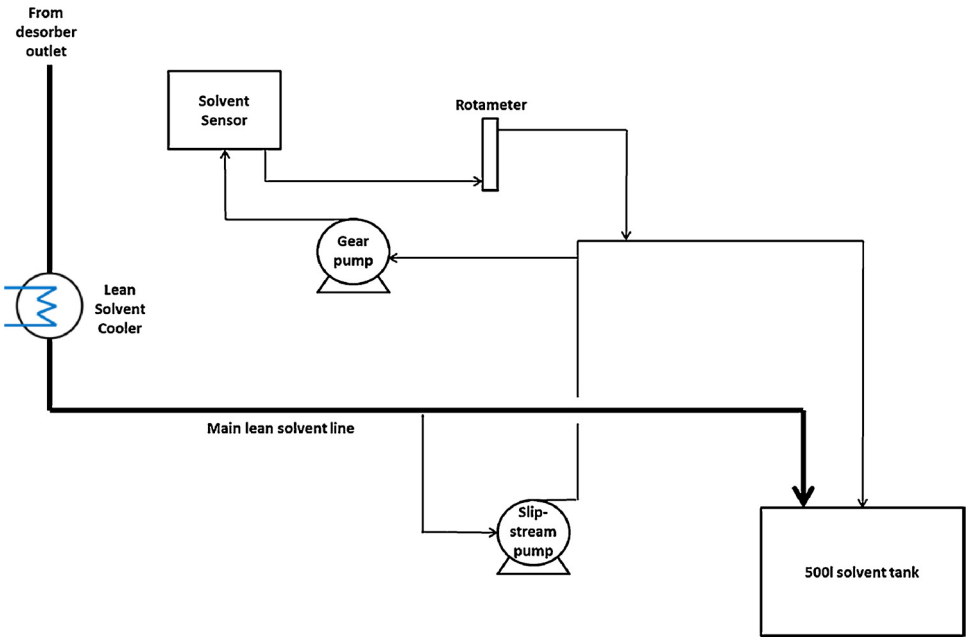

Fig. 4. Liquid loop for online solvent sensor – location upstream of solvent tank.

The time shifting method predicts that only the first lean solvent "packet" sampled at $t = 0$ will reach the absorber inlet before the end of this scenario. Subsequent lean solvent samples were not given sufficient time to reach the absorber inlet. To observe the increase in solvent loading at the rich loading sampling port, the solvent could have be allowed to circulate for a longer period of time, with lean and rich samples taken at more regular intervals in order to observe the full convergence of lean and rich loading as the solvent continues to circulate.

5.2. Gas turbine startup

Due to the nature of the shutdown sequence, which involves a continued circulation of solvent at 30% of baseload in order to lower solvent temperature more rapidly, and consequently an equilibration of solvent loadings due to mixing, the startup sequence is initiated with lean loading and rich loading, respectively, higher and lower than baseload values at baseload conditions.

Gas flow is initiated at $t = 0$ and increased at a rate of 5.7% of baseload/min. Once the flow of gas reaches 30%, at approx. $t = 5$ min 15 s, the flow rate of liquid commences ramping at 5.7%/min in order to maintain a constant L/G flow ratio.

As suggested by the models of Ceccarelli et al. (2014), the CO_2 capture rate (Fig. 8c) is initially higher than that of baseload operation between $t = 0$ and approximately $t = 5$ min, as the gas flow rate is ramped up to reach the operating liquid to gas ratio of the absorber. With the holdup on the packing already established, a cool solvent also results in a higher driving force for CO_2 absorption. Once

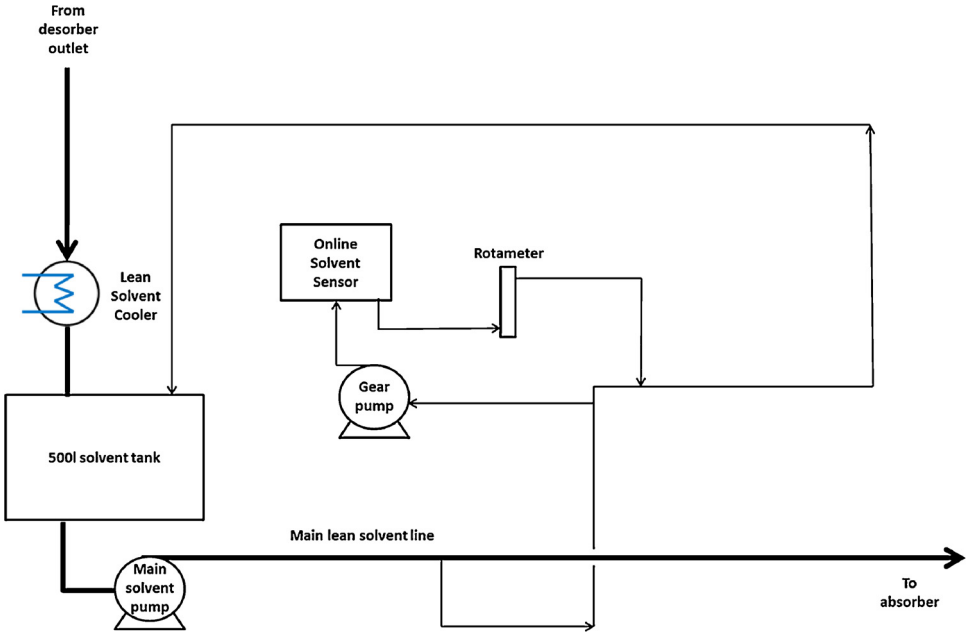

Fig. 5. Liquid loop for online solvent sensor – downstream of solvent tank.

Please cite this article in press as: Tait, P., et al., A pilot-scale study of dynamic response scenarios for the flexible operation of post-combustion CO_2 capture. Int. J. Greenhouse Gas Control (2015), http://dx.doi.org/10.1016/j.ijggc.2015.12.009

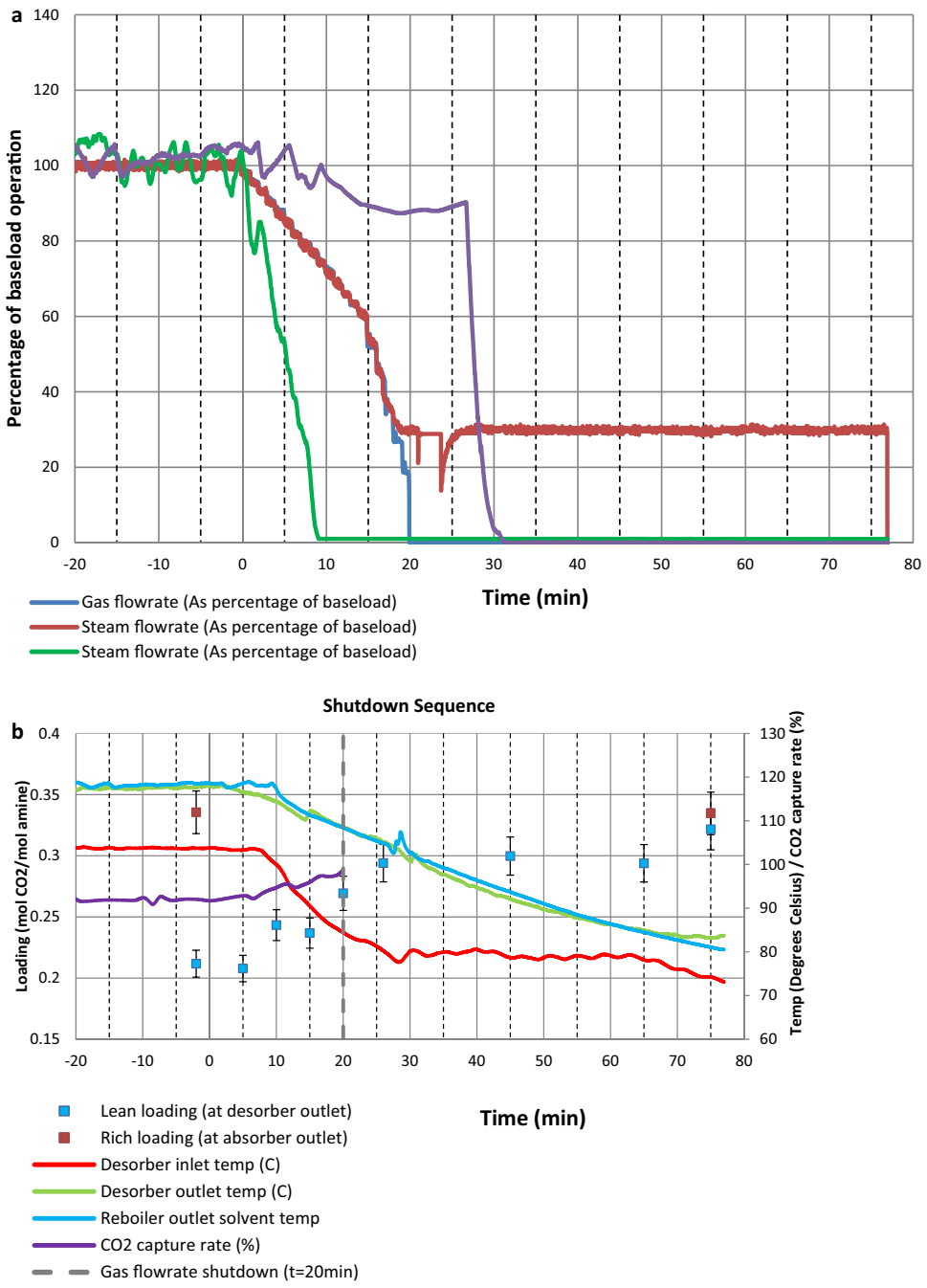

Fig. 6. (a) Gas, liquid and steam flow rates as percentage of previously-defined baseload operation, gas turbine shutdown sequence. (b) Rich and lean solvent CO2 loading, CO_2 capture rate, desorber and reboiler temperatures, gas turbine shutdown sequence.

the target liquid/gas flow ratio is established at $t = 5$ min and the absorber temperature profile increases in magnitude (Fig. 9a), the capture rate begins to drop due to the lean solvent loading becoming gradually higher than at baseload operation, resulting in a lower driving force for the absorption of CO_2 (Fig. 8c).

At $t = 11$ min, ramp rates of both liquid and gas flow rates are decreased to approx. 2.45%/min and retained at this value until both reach 100% of baseload, at around $t = 26$ min. Steam flow rate is ramped at a rate of 18.0%/min from $t = 15$ to $t = 18$ min, before the ramp rate is decreased to approx. 2.55%/min. The manual valve controlling desorber pressure is closed at $t = 17$ min. Although the flow of steam to the reboiler is established and stabilised at 100% of baseload by $t = 35$ min, the steam flow to the rich solvent heater (which is used to simulate the effect of the cross-flow heat exchanger) is not initiated until $t = 60$ min (Fig. 8b), due to an error by the plant operator. The capture rate continues to decrease until solvent which has been exposed to standard desorber operation circulates through the liquid tank and pipework to the absorber inlet.

This was not identified until after the conclusion of the test campaign, but the data is included since valuable information can still be gained from this scenario.

Until $t = 60$ min, a significant fraction of the thermal input from the reboiler contributes to increasing the temperature of incoming solvent to the desorber by an additional 50–60 °C compared to baseload operation, and energy which could otherwise be used to strip CO_2 is lost as sensible heat.

Please cite this article in press as: Tait, P., et al., A pilot-scale study of dynamic response scenarios for the flexible operation of post-combustion CO_2 capture. Int. J. Greenhouse Gas Control (2015), http://dx.doi.org/10.1016/j.ijggc.2015.12.009

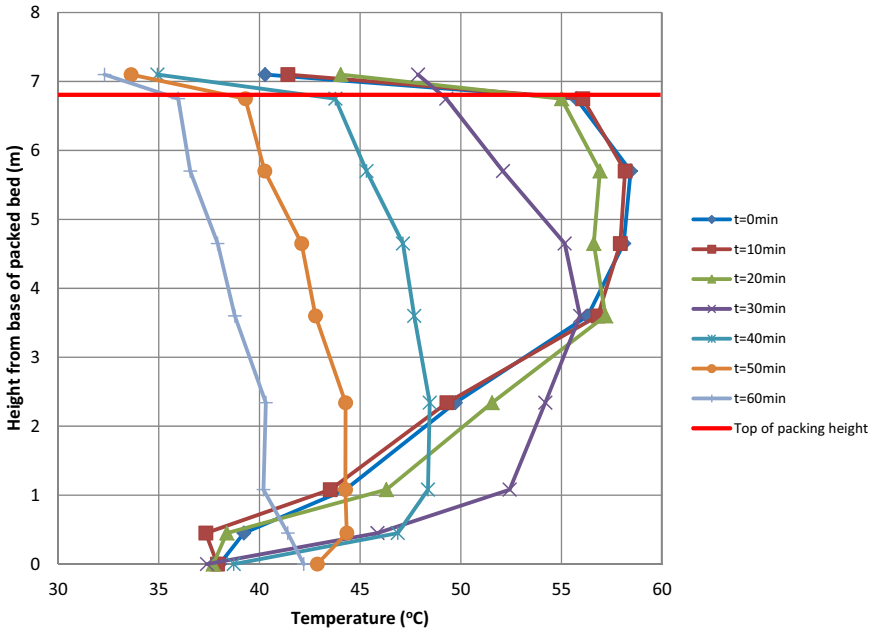

Fig. 7. Evolution of absorber temperature profile during gas turbine shutdown operation.

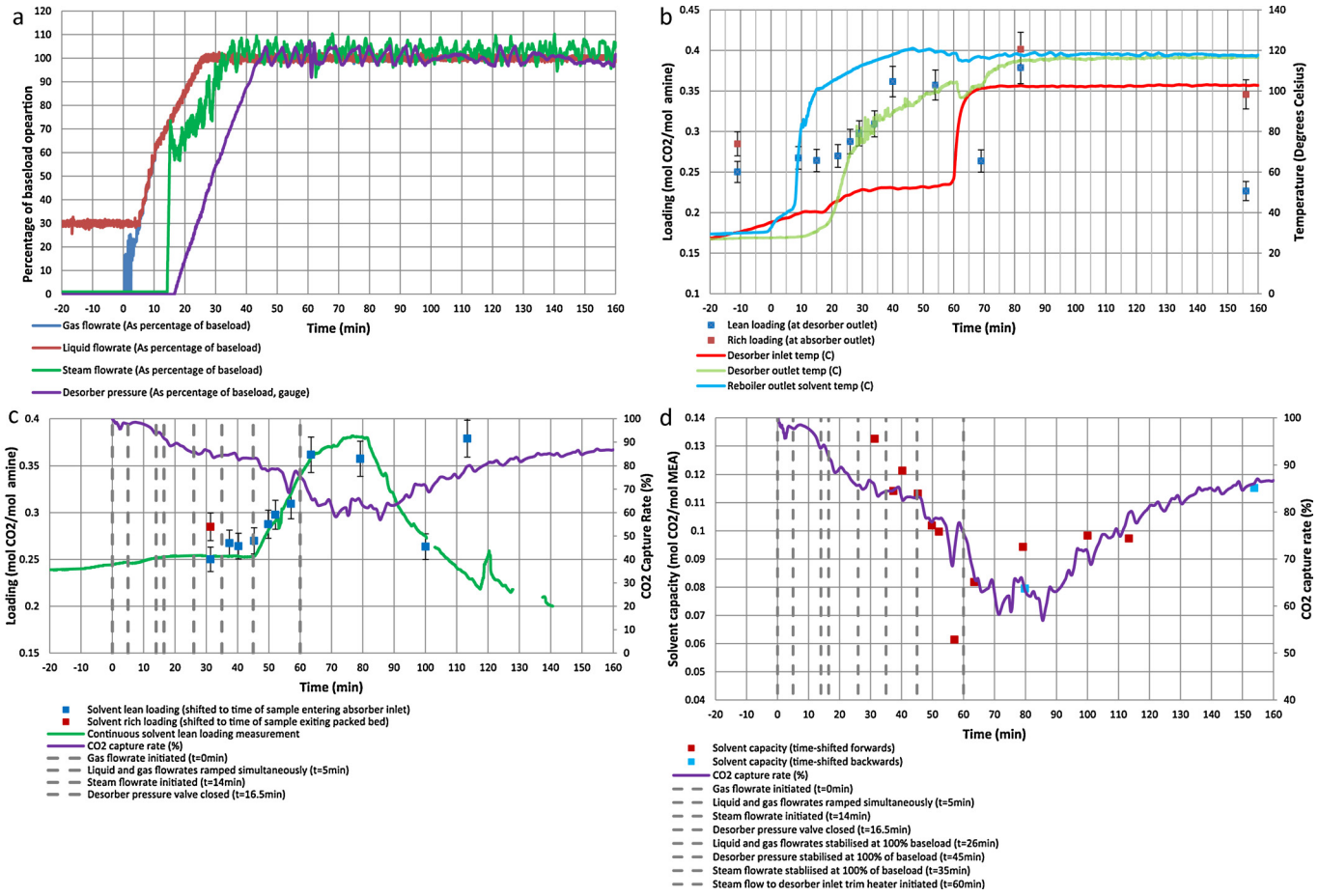

Fig. 8. (a) Gas, liquid and steam flow rates as percentage of previously-defined baseload operation, gas turbine startup scenario. (b) Rich and lean solvent CO_2 loading at sampling ports, desorber and reboiler temperatures, gas turbine startup scenario. (c) Lean and rich solvent loading titration measurements, shifted to time of absorber inlet entry and outlet exit respectively, continuous lean loading measurement, CO_2 capture rate, gas turbine startup scenario. (d) Predicted real-time solvent capacity and CO_2 capture rate, gas turbine startup scenario.

Please cite this article in press as: Tait, P., et al., A pilot-scale study of dynamic response scenarios for the flexible operation of post-combustion CO_2 capture. Int. J. Greenhouse Gas Control (2015), http://dx.doi.org/10.1016/j.ijggc.2015.12.009

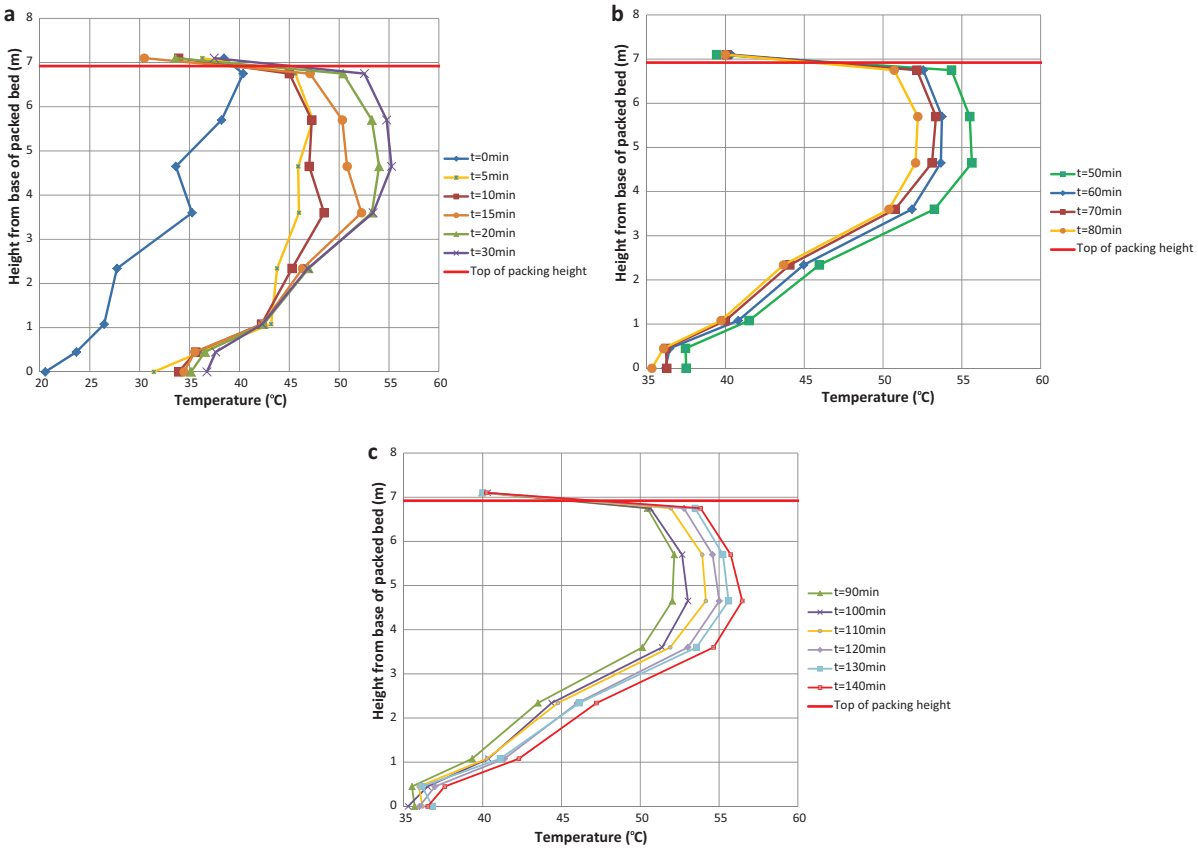

Fig. 9. (a) Evolution of absorber temperature profile, $t = 0$ min – $t = 30$ min, gas turbine startup scenario. (b) Evolution of absorber temperature profile, $t = 50$ min – $t = 80$ min, gas turbine startup scenario. (c) Evolution of absorber temperature profile, $t = 90$ min – $t = 140$ min, gas turbine startup scenario.

As a consequence, the lean loading gradually increases to around 0.36 mol CO_2/mol MEA which compromises the driving force and solvent capacity in the absorber column, as shown in Fig. 8d. This results in a gradual drop in capture level down to around 65% from $t = 65$ min to $t = 90$ min.

Interestingly, this effect is somewhat less pronounced than what would be expected for an absorber configuration optimised for natural gas equivalent CO_2 concentrations, since the pilot plant facility is operated with a lower rich loading. As a result there is additional margin for the rich loading to increase before a pinch in absorption is reached at the bottom of the absorber.

The decrease in absorber temperature profile (Fig. 9b) can be directly linked to this decrease in capture rate, both of which reach a minimum at $t = 80$ min. Leaner solvent which has been exposed to baseload desorber and reboiler operation is returned to the absorber after $t = 80$ min (Fig. 8c and d), resulting in a higher driving force for CO_2 absorption and a steady increase in capture rate (Fig. 8c and d) and absorber temperature (Fig. 9c). The capture rate, predicted solvent capacity and continuous lean solvent loading measurement all suggest a steady decrease in solvent lean loading at the absorber inlet after $t = 80$ min, so it is believed that the bench lean loading measurement of 0.3787 at $t = 113$ min (Fig. 8c) is the result of an abnormal or unrepresentative titration measurement. Triplicate analysis of 14 samples taken over the course of the test campaign resulted in an estimated uncertainty of 5.2%, suggesting that the source of the error most likely lies within the sample, and not the titration method. The sample may be an example of abnormal "noise" and therefore unrepresentative of overall change, or the result of unknown mixing effects in the desorber sump. Several similar measurements are encountered throughout the test campaign, and unfortunately it is not possible to know definitively the source of the abnormal measurement without more regular sampling.

The outcomes from this experiment suggest that a decrease in capture rate following startup is inevitable as plant parameters stabilise, in cases where some solvent flow rate has been maintained between the shutdown and startup to use the cooling capacity available. If maintaining a high capture rate is of critical importance, interim solvent storage has been proposed as a method to increase capture flexibility, by ensuring that a large separate reserve of lean solvent is available until the plant is stabilised at baseload (Lucquiaud et al., 2014).

5.3. Power output maximisation by capture plant decoupling

Before the capture plant decoupling scenario is initiated, the plant is operating at steady state baseload. The flow rates of steam and gas are reduced to zero at $t = 0$ min and $t = 1$ min, respectively, with the capture rate dropping to zero shortly thereafter, at $t = 2.5$ min, since gas no longer passes through the absorber. The manual valve maintaining pressure in the desorber is released at $t = 8$ min to prevent creation of vacuum in the desorber. The flow of liquid is turned down in two steps, to 75% of baseload at $t = 9$ min, then 50% at $t = 14$ min. Solvent flow is maintained at 50%, reproducing likely operating conditions where power for solvent circulation is reduced to a minimum to maximise electricity power output. Maintaining a minimum solvent flow rate also allows, if necessary, for fast startup of the capture plant than turning off the solvent pumps. This lower solvent flow rate, combined with a constant solvent cooling capacity, ensures that a substantial reserve of solvent capacity is available so that capture rate can rapidly return

Please cite this article in press as: Tait, P., et al., A pilot-scale study of dynamic response scenarios for the flexible operation of post-combustion CO_2 capture. Int. J. Greenhouse Gas Control (2015), http://dx.doi.org/10.1016/j.ijggc.2015.12.009

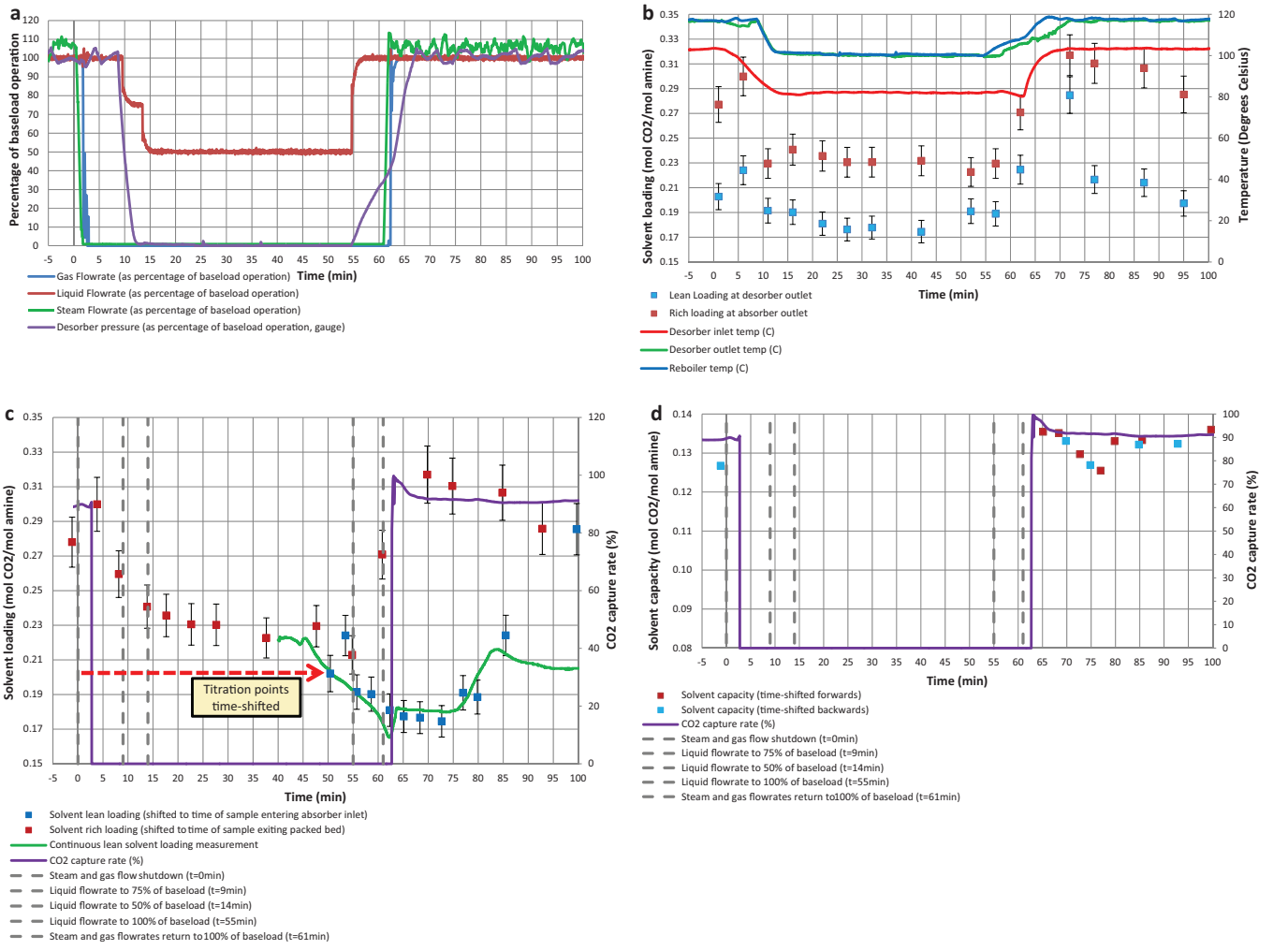

Fig. 10. (a) Gas, liquid and steam flow rates as percentage of previously-defined baseload operation, power output maximisation by capture plant decoupling scenario. (b) Rich and lean solvent CO2 loading at sampling ports, desorber and reboiler temperatures, power output maximisation by capture plant decoupling scenario. (c) Lean and rich solvent loading titration measurements, shifted to time of absorber inlet entry and outlet exit respectively, continuous lean loading measurement, CO_2 capture rate, power output maximisation by capture plant decoupling scenario. (d) Predicted real-time solvent capacity and CO_2 capture rate, power output maximisation by capture plant decoupling scenario. (For interpretation of the references to color in the text, the reader is referred to the web version of the article.)

to normal levels upon reintroduction of flue gas to the absorber column.

Lean solvent loading measured via titration at the desorber outlet appears to rise between $t = 1$ min and $t = 6$ min, before dropping once again at $t = 11$ min. The rise in lean loading around $t = 6$ min is not observed in the continuous measurement, which indicates that this sample may be unrepresentative of plant trends, as discussed at the end of Section 5.1. The liquid flow rate is still operating at 100% until $t = 9$ min, and by the time the sample at $t = 11$ is taken, solvent which has not been exposed to CO_2 in the absorber begins to appear at the desorber outlet. This is consistent with the circulation time between the top of the absorber sump and top of the desorber sump at $L = 100\%$ being approx. 8 min in total, allowing 6 min from absorber outlet to desorber, plus an additional 2 min to pass through the desorber sump.

After the flow of gas has been shut down, the absorber temperature bulge decreases in magnitude and moves down the column as hot solvent in the upper region of the absorber flows down the packed bed, being replaced by colder solvent as liquid (Fig. 11a). The absorber is insulated and requires some time to cool down, as heat is transferred from the packing to the incoming cool solvent.

Assuming that the lean titration measurement at $t = 6$ min is anomalous and unrepresentative of true plant trends, lean loading at the desorber outlet sampling port decreases from 0.202 mol/mol to 0.174 mol/mol from $t = 0$ min until around $t = 50$ min (Fig. 10b) as residual heat in the desorber continues to liberate small amounts of CO_2, from solvent not exposed to CO_2 in the absorber.

Lean loading titration measurements taken from $t = 0$ min are shifted forward to the time of entry of the corresponding packet of solvent to the absorber inlet (blue markers) in Fig. 10c. The continuous online solvent measurement shows good agreement with the titration data until $t = 85$ min. Based on the liquid flow rate and volume of liquid in the pipework between the lean solvent sampling port and absorber inlet, the lean loading value of 0.204 mol/mol at $t = 1$ min (Fig. 10b), is predicted to reach the absorber inlet at $t = 54$ min (Fig. 10c). This appears very close to the rich loading value of 0.213 mol/mol, corresponding to the time of exit of the absorber outlet at $t = 54$ min. Given that there is no CO_2 flow into the absorber between $t = 1$ min and $t = 54$ min, this indicates that the time-shifting method provides a moderately accurate estimation of solvent circulation time of 53 min. This is also roughly consistent with the estimated circulation time of 63 min at 50% of baseload flow rate shown in Table 3, given than titration measurements are taken every 5 min and that the solvent flow rate does not reach 50% of baseload for the first 15 min.

Please cite this article in press as: Tait, P., et al., A pilot-scale study of dynamic response scenarios for the flexible operation of post-combustion CO_2 capture. Int. J. Greenhouse Gas Control (2015), http://dx.doi.org/10.1016/j.ijggc.2015.12.009

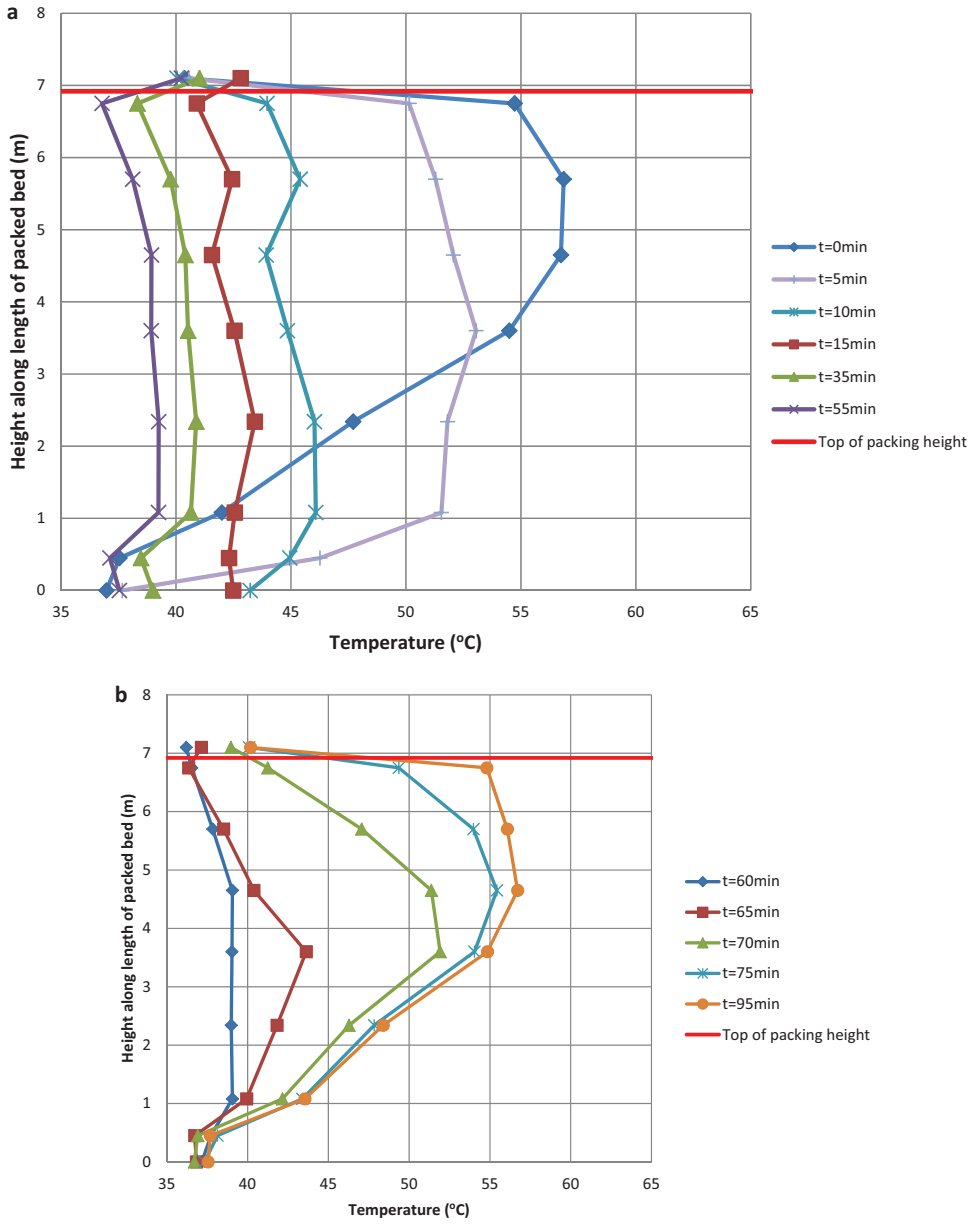

Fig. 11. (a) Evolution of absorber temperature profile during power output maximisation by capture plant decoupling scenario – temperature decrease. (b) Evolution of absorber temperature profile during power output maximisation by capture plant decoupling scenario – temperature increase.

The temperature profile of the absorber (Fig. 11a) decreases in magnitude after $t = 0$ min, as the exothermic absorption of CO_2 stops after the flow rate reaches zero. The absorber temperature bulge exhibits a similar response to that observed during simulated gas turbine shutdown, decreasing in magnitude and moving down the packing height as hot solvent flows down the packed bed and is replaced by slow flowing incoming cooler solvent. By $t = 15$ min there is no observable bulge, and the temperature across the entirety of the packed bed decreases until flue gas is reintroduced.

The desorber manual release valve is closed and pressure begins to rise at $t = 55$ min. At $t = 60$ min, the bypass event ends and the flow rates of gas and steam are ramped back up to 100%.

Rich loading increases rapidly upon reintroduction of CO_2 to the absorber at $t = 62$ min. The capture rate is initially higher than the baseload value as a batch of cool solvent promotes CO_2 absorption, and this is reflected in the rich loading titration measurements of 0.316, 0.313, 0.306 mol/mol at $t = 72$, 77 and 87 min (respectively Fig. 10b). The lean loading at the desorber outlet follows a similar trend once the desorber has reached operational temperature, with the circulation time from the absorber sump to the desorber sump being around 6 min at 100% baseload solvent flow rate. A temperature bulge is observed in the absorber at $t = 65$ min, 3 min after the reintroduction of gas flow, and is fully established by $t = 95$ min.

Fig. 10c shows the lean and rich solvent measurements time-shifted to the absorber inlet and outlet. It should be noted that the time-shifting method detailed in Section 3.4 contains a level of uncertainty due to the hydraulic response of the plant, and in this case predicts an increase in solvent loading at the base of the absorber packing at $t = 61$ min, 60 s before the flow of gas is reintroduced. A batch of richer lean solvent which is predicted to reach the inlet between $t = 85$ and $t = 99$ min appears not to be detected by the online solvent sensor, and has no real effect on the capture rate. It is possible that there is sufficient mixing with leaner solvent between the sampling port and the absorber inlet, that the increase in

Please cite this article in press as: Tait, P., et al., A pilot-scale study of dynamic response scenarios for the flexible operation of post-combustion CO_2 capture. Int. J. Greenhouse Gas Control (2015), http://dx.doi.org/10.1016/j.ijggc.2015.12.009

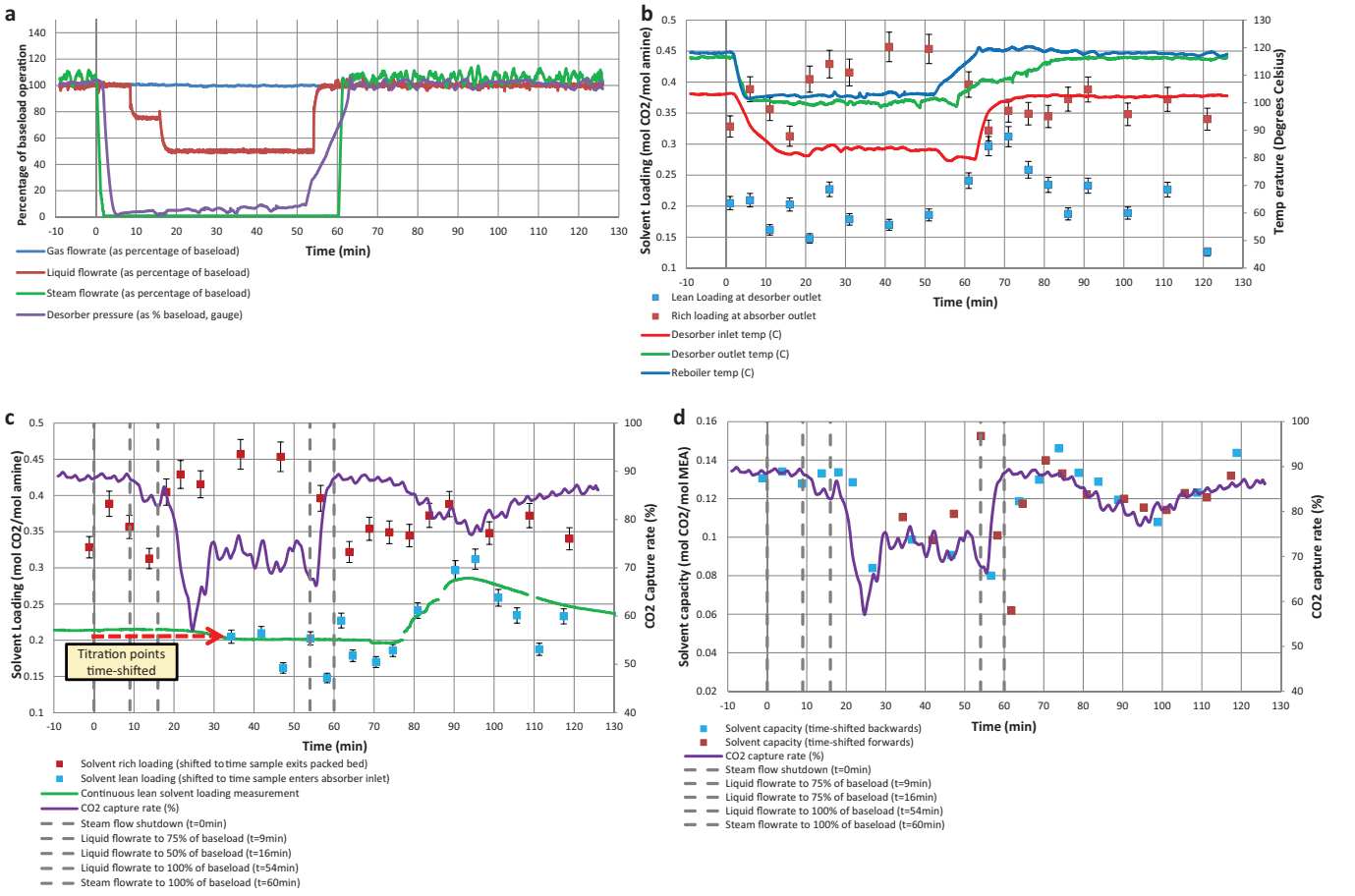

Fig. 12. (a) Gas, liquid and steam flow rates as percentage of previously-defined baseload operation, for power output maximisation by reboiler steam decoupling scenario. (b) Rich and lean solvent CO_2 loading at sample points, desorber and reboiler temperatures, power output maximisation by reboiler steam decoupling scenario. (c) Rich and lean solvent loading bench measurements, time-shifted to absorber inlet and outlet respectively, continuous lean loading measurement, CO_2 capture rate, power output maximisation by steam decoupling scenario. (d) Predicted real-time solvent capacity and CO_2 capture rate, power output maximisation by steam decoupling scenario.

loading is dampened. It is also possible that the titration measurement at $t = 72$ min (Fig. 10b)/$t = 99$ min (Fig. 10c) is unrepresentative of plant conditions, as discussed in Section 5.1.

The time shifting method is used to show the solvent working capacity in the absorber, in mol/mol (Fig. 10d), and how it correlates to capture level. Solvent working capacity is calculated as described in Section 3.4.

In this scenario there is no observable reduction in capture rate upon reintroduction of flue gas. However, it is worth noting that the effect on capture rate upon reintroduction of flue gas will be highly dependent on the length of the shutdown operation, the circulation time, total solvent inventory and extent of mixing in the liquid loop for each individual capture plant.

Potential detrimental effects on capture rate upon restart could be mitigated by using interim solvent storage. This involves holding a batch of lean solvent in reserve so it can be fed to the absorber while the original solvent is being regenerated. The stored lean solvent can also be used to replace the original which is diverted to a rich solvent storage tank for future regeneration when energy selling price is low.

5.4. Power output maximisation by reboiler steam decoupling only

Although similar to the previous scenario, a significant difference is that flue gas is continuously fed to the absorber column during reboiler steam shutdown. Steam flow to the reboiler is reduced to zero at $t = 0$ min, followed by the opening of the desorber pressure release valve at $t = 1$ min. Solvent flow rate is turned down to 75%, then 50% at $t = 8$ min and $t = 15$ min respectively. The capture rate begins to drop at $t = 8$ min after the initial decrease in solvent flow, but does not decrease sharply until $t = 17$ min.

Lean loading at the desorber outlet appears to fluctuate between $t = 6$ and $t = 31$ min, based on the titration measurements taken. When the flow rate of solvent is reduced rapidly, the PID control system may fully close the desorber outlet valve for several minutes in an attempt to maintain desorber sump level. Solvent which has not been exposed to steam flow will have ample opportunity to mix with fully regenerated solvent in the desorber sump. This mixing effect makes it very difficult to predict what will happen to the lean loading at the desorber outlet, although based on the results from the online solvent sensor, it is possible that the titration measurements at $t = 11$ and $t = 21$ min are abnormal or unrepresentative of the lean solvent loading which will be seen by the solvent sensor, due to mixing effects in the main solvent tank.

In this and the final dynamic scenario (Section 5.5), the online solvent sensor is relocated to just downstream of the main solvent pump. Interestingly, when the continuous measurement output and titration values are shifted to the time at which each packet of solvent would reach the absorber inlet (Fig. 12c), this fluctuating lean loading behaviour is not observed. This may suggest that the fluctuations in lean solvent loading at the desorber are dampened due to mixing in the solvent tank, and will not have a considerable impact on the lean loading at the absorber inlet.

Please cite this article in press as: Tait, P., et al., A pilot-scale study of dynamic response scenarios for the flexible operation of post-combustion CO_2 capture. Int. J. Greenhouse Gas Control (2015), http://dx.doi.org/10.1016/j.ijggc.2015.12.009

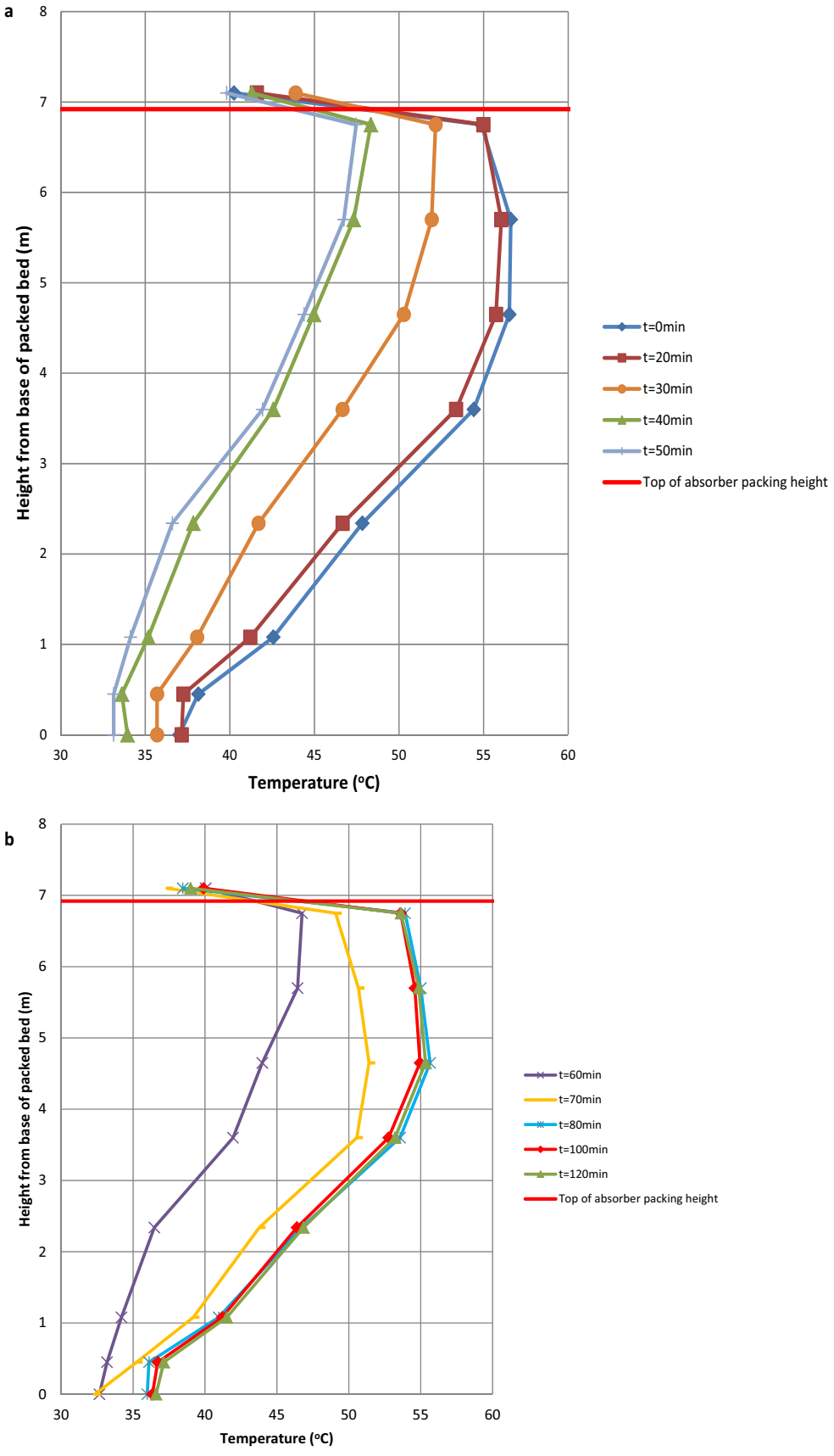

Fig. 13. (a) Evolution of absorber temperature profile, power output maximisation by reboiler steam decoupling scenario – temperature decrease. (b) Evolution of absorber temperature profile, power output maximisation by reboiler steam decoupling scenario – temperature increase.

Please cite this article in press as: Tait, P., et al., A pilot-scale study of dynamic response scenarios for the flexible operation of post-combustion CO_2 capture. Int. J. Greenhouse Gas Control (2015), http://dx.doi.org/10.1016/j.ijggc.2015.12.009

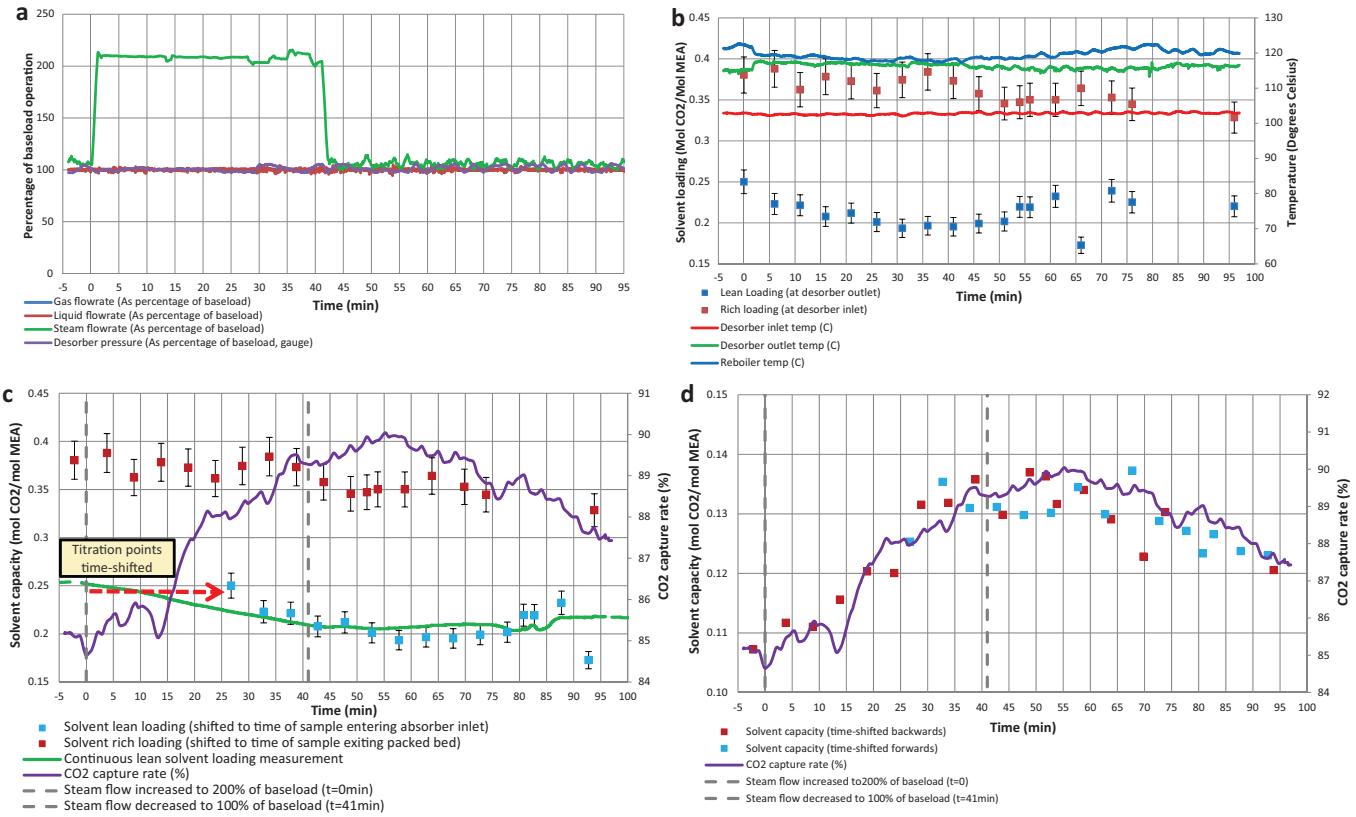

Fig. 14. (a) Gas, liquid and steam flow rates as percentage of previously-defined baseload operation, frequency response scenario. (b) Rich and lean solvent CO_2 loading, desorber and reboiler temperatures frequency response scenario. (c) Lean and rich solvent loading bench measurements, time-shifted to absorber inlet and outlet respectively, continuous lean loading measurement, CO_2 capture rate, frequency response scenario. (d) Predicted real-time solvent capacity and CO_2 capture rate, frequency response scenario.

The general trend in rich loading at the absorber outlet before the flow rate of liquid is ramped back up to 100% at $t = 53$ min is an increasing one (Fig. 12b). This is a direct result of the decreased L/G flow ratio, down from 2.86 at baseload to 1.43 from $t = 17$ min, and the increased liquid residence time on the packing, which results in additional CO_2 being absorbed per unit of solvent flowing into the column. Although the rich solvent loading at the bottom of the absorber increases, the liquid flow rate is low enough that the amount of CO_2 captured is reduced overall. The absorber temperature bulge decreases in magnitude (Fig. 13a), consistent with the decrease in capture rate, and moves upwards. The upwards shift may be due to diminished working capacity, capture rate and L/G ratio, which results in higher concentrations of CO_2 in the upper regions of the absorber. The solvent becomes loaded with CO_2 more rapidly upon entry, decreasing the driving force for CO_2 absorption as it flows down the packed bed. Higher CO_2 concentration in the upper regions of the packing also results in a higher driving force for CO_2 absorption on the gas-side.

The desorber pressure release valve is closed and liquid flow ramped back up at $t = 52$ and 53 min, respectively, in anticipation of the plant returning to normal operating conditions. Steam flow is ramped back up to 100% at $t = 60$ min. In total, the steam shutdown operation lasts 60 min, a plausible duration for a bypass in response to an evening peak in electricity prices. Lean loading at the desorber outlet decreases between $t = 71$ and $t = 76$ min, once the desorber reaches operational temperature (Fig. 12b). The estimated real-time solvent loading capacity (Fig. 12d) appears to follow the capture rate for the majority of the scenario, except for two points at $t = 54.07$ and 61.08. This may be due to the fact that the lean loading titration measurements, which the calculations are based on, are erroneous or that the CO_2 flow rate into the absorber is not entirely stable during this time, with the mass flow controller aiming to maintain a steady CO_2 concentration at the absorber inlet while the capture rate and concentration of CO_2 in the recycled flue gas stream is highly variable.

Capture rate is observed to decrease between $t = 75$ and $t = 95$ min, corresponding to the time at which solvent not fully regenerated in the desorber is predicted to reach the absorber inlet (Fig. 12c).

There is good agreement around $t = 95$ min between solvent working capacity and capture rate, yet, in Fig. 12c, the lean loading value of 0.312 mol/mol, time shifted to $t = 95$ min, is close to the rich loading value of 0.348 mol/mol while a capture rate of >75% is achieved. This is considerably higher than the baseload lean loading value of 0.232 mol MEA/mol CO_2 (Section 3.1) As mentioned in Section 3.4, the time shifting method is not able to account for mixing effects, since it relies on the assumption of plug flow. This illustrates that it is likely that mixing effects in the solvent tank, located between the lean and the rich sampling points, play an important role to maintain solvent working capacity and capture rate around 75–80% for 20–25 min from $t = 75$ min onwards.

The batch of richer lean solvent passing through the absorber, indicated by the online measurement lean loading readings in Fig. 12c at around $t = 95$ min, is then followed by a rise in capture rate before the plant returns to steady state baseload operation. The absorber temperature bulge reflects the evolution of the capture rate, increasing in magnitude and moving down the packing height after $t = 60$ min (Fig. 13b). The temperature profile decreases slightly around $t = 100$ min, coinciding with the drop in capture rate, before increasing as the plant reaches steady state operation

Please cite this article in press as: Tait, P., et al., A pilot-scale study of dynamic response scenarios for the flexible operation of post-combustion CO_2 capture. Int. J. Greenhouse Gas Control (2015), http://dx.doi.org/10.1016/j.ijggc.2015.12.009

at $t = 120$ min. This decrease in capture rate observed 20 min after the supply of thermal energy to the reboiler is resumed could be avoided by using interim solvent storage.

A thorough understanding of plant circulation times, combined with continuous monitoring of solvent loading at the liquid inlet and outlet of the absorber would allow operators to anticipate this decrease in capture rate and compensate accordingly by anticipating to adjust solvent working capacity.

5.5. Frequency response by rapid reboiler steam flow increase

The flow rate of steam to the reboiler is increased rapidly to 200% at $t = 0$ and remains at this value for 41 min, while all other plant parameters remain constant. Plant data continue to be obtained for an additional 50 min after steam had been ramped down, in order to observe any further effects on the response of the plant.

It is important to note that the plant may not have fully reached a steady-state operating condition at the start of this scenario, with the initial capture rate at 85% and a lean loading of 0.250 mol/mol.

Lean loading at the desorber outlet is observed to decrease steadily from 0.250 mol/mol after the flow rate of steam is increased at $t = 0$, eventually stabilising at around 0.2 mol CO_2/mol amine (Fig. 14b). These titration data are shifted to the time at which each sample would reach the absorber inlet in Fig. 14c. The online solvent sensor output displays similar behaviour, but the decrease in lean loading appears less rapid. As the sensor is located after the main solvent tank, any rapid changes in lean loading at the desorber outlet are dampened when that packet of solvent reaches the sensor, due to mixing in the solvent tank, as previously explained. The continuous measurement suggests that the lean loading at the absorber inlet begins to decrease before any solvent which has undergone a greater degree of regeneration due to increased steam flow is expected to reach the absorber inlet. As the plant is not initially at baseload, it is not possible to attribute the observed increase in capture rate and decrease in lean loading at the absorber inlet between $t = 0$ and $t = 25$ min to the frequency response operation.

Fig. 14c and d shows that, when solvent which has undergone a greater degree of regeneration due to increased steam flow starts entering the absorber from $t = 26$ min onwards, the increase in solvent working capacity results in an increase in capture rate from 88% to 90%. Steam flow is turned down to 100% of baseload at $t = 41$ min. The response of the capture rate, starting at $t = 70$ min, corresponds to an increase in lean solvent loading at the absorber inlet (Fig. 14c).

A titration lean loading measurement at $t = 66$ min (Fig. 14b)/$t = 93$ min (Fig. 14c) appears to be anomalous as there is no significant change in the capture rate, and it deviates significantly from the online lean loading measurement at this point in time.

The calculated real-time solvent working capacity (Fig. 14d) follows well the trend of the capture rate over the course of the whole experiment. Accurate monitoring and prediction of real-time working capacity via continuous loading measurements at the absorber inlet and outlet could prove to be a key metric in future advanced control systems for dynamic post-combustion capture.

As there is no significant change in absorber temperature profile, the maximum dT over the course of the experiment being an increase of 1.68 °C at height of 3.6 m, absorber temperature data are not reported for this scenario.

6. Conclusions

Five enhanced operational flexibility scenarios of an amine post-combustion capture process treating flue gas from a state of the art combined cycle gas turbine plant are investigated in this work.

No significant barriers to flexible operation were observed for this pilot facility. It is possible that plants operated with higher rich loadings at baseload would have a more limited capacity to absorb CO_2 in the absence of heat input for regeneration, which may result in a more rapid drop-off in capture rate. Solvent inventory and circulation times are observed to have a significant effect on capture rate during certain dynamic operations, with longer circulation times resulting in the plant requiring additional time to return to steady-state following a perturbation. Indeed, if the capture plant is required to operate in continuously changing scenarios, for example load-following, it may never return to steady-state operation.

A reduction of solvent inventory may help to reduce delays due to circulation times, but there are positive effects in having a large solvent inventory – this increases the solvent capacity of the plant, and as observed in one of the two scenarios for power output maximisation, it allows the plant to maintain a CO_2 capture rate greater than 55%, and around 75% for most of the duration of the 60 min whilst steam supply to the reboiler is turned off.

For optimum performance in electricity markets, anecdotal evidence suggests that altering power output every 30 min is desirable, e.g. 30 min is the duration of settlement period in the Balancing and Settlement Code for electricity generation in the UK. Flexible operation can also be of benefit to baseload generation plants equipped with CCS, as they can modify capture rate and electricity output in response to market fluctuations in CO_2 and electricity selling price (Mac Dowell and Shah, 2014).

For the process control loop of an amine post-combustion capture process, this would require solvent loading measurements to be performed continuously if they are to be used as a control variable. An automated control system must perform feedback control loop operations at least 10× faster than the time frame required to change state. Therefore, if the capture plant changes state once every 30 min, the feedback operation must be performed at least once every 3 min. Obtaining a solvent loading measurement within this timeframe is not possible with existing methods – manual sampling followed by loading analysis at regular intervals is time-consuming and labour-intensive, while anecdotal evidence regarding the use of automated titration systems indicates that each loading measurement procedure can take up to 20 min.

The implementation of an online solvent sensor for continuous real-time measurements of lean solvent loading during this test campaign proved a successful step in reducing the time required to obtain solvent loading measurements. Model predictive control has been identified as a method by which PCC could react to perturbations optimally (Mechleri, 2015), and accurate, continuous loading measurements at the absorber inlet and outlet are likely to be key control variables (Seibert et al., 2011; van der Ham et al., 2014). A further online measurement of loading at the desorber outlet, combined with extensive knowledge of plant circulation times and mixing effects, would allow for greater control over capture rates due to more accurate prediction of solvent loading at the absorber inlet.

Although the sensor performed adequately during this test campaign, there still exists scope for improvement. Current efforts aim to improve sensor stability as rapid changes in solvent loading can result in software errors. Automated data-logging capability will also be added and the sensor will be redesigned for industrial field deployment.

This work indicates that a potential solution to the problem of reduced CO_2 capture as a result of certain dynamic operations is to actively manage solvent inventory. For example, flow rates and/or loadings, combined with forewarning of changes in power plant output and an appropriate control system could allow for the mitigation of detrimental impacts on performance. An option proposed previously is the use of two additional tanks, both separated from the rest of the liquid loop by valves. One tank could contain a reserve of lean solvent to be utilised during steam

Please cite this article in press as: Tait, P., et al., A pilot-scale study of dynamic response scenarios for the flexible operation of post-combustion CO_2 capture. Int. J. Greenhouse Gas Control (2015), http://dx.doi.org/10.1016/j.ijggc.2015.12.009

shutdown situations, while the second tank could act as a receptacle for excess rich solvent, as initially suggested by (Chalmers and Gibbins, 2007) and widely studied since by others, e.g. (Chalmers et al., 2009; Oates et al., 2014). An alternative proposed by Mac Dowell and Shah (2014) is to vary solvent regeneration levels in anticipation of future power plant output, although this work shows that mixing in the solvent line between the reboiler and absorber inlet will affect lean loading for a short period of time after the level of regeneration is changed.

The added flexibility made available by either method is one benefit of post-combustion capture, and combined with the further development of real-time solvent loading measurement options, is a worthy subject for future investigation at pilot plant scale.

Acknowledgements

The authors would like to thank Sulzer ChemTech and the Energy Technology Partnership (ETP) for financial support to Paul Tait. Financial and technical support for the operation of the pilot-scale facility from Sulzer ChemTech is also gratefully acknowledged, and financial support from a UK Carbon Capture Research Centre funded project (UKCCSRC-C2-214), the EPSRC (EP/J020788/1) and the Royal Academy of Engineering for equipment. The online sensor used in this work was developed with funding from Doosan Power Systems and the Energy Technology Partnership (ETP). This research was carried out as part of the UKCCSRC's GAS-FACTS project.

Appendix A. Supplementary data

Supplementary data associated with this article can be found, in the online version, at doi:10.1016/j.ijggc.2015.12.009.

References

Artanto, Y., Jansen, J., Pearson, P., Do, T., Cottrell, A., Meuleman, E., Feron, P., 2012. Performance of MEA and amine-blends in the CSIRO PCC pilot plant at Loy Yang Power in Australia. Fuel 101, 264–275.
Biliyok, C., Mechleri, E.D., Thornhill, N.F., 2014. Dynamic simulation and control of post-combustion CO_2 capture with MEA in a gas fired power plant. Comput. Aided Chem. Eng. 33, 619–624.
Bui, M., Gunawan, I., Verheyen, V., Artanto, Y., Meuleman, E., Feron, P., 2013. Dynamic modelling and validation of post-combustion CO_2 capture plants in Australian coal-fired power stations. Energy Procedia 37, 2694–2702.
Bui, M., Gunawan, I., Verheyen, V., Feron, P., Meuleman, E., Adeloju, S., 2014. Dynamic modelling and optimisation of flexible operation in post-combustion CO_2 capture plants – a review. Comput. Chem. Eng. 61, 245–265.
Carey, J., Damen, K., Fitzgerald, F.D., Gardiner, R.A., 2013. CCPilot 100+ operating experience and test results. Energy Procedia 37, 6170–6178.
Ceccarelli, N., van Leeuwen, M., van Leeuwen, P., Maas, W., Ramos, A., van der Vaart, R., Wolf, T., 2014. Flexibility of low-CO_2 gas power plants: integration of the CO_2 capture unit with CCGT operation. Energy Procedia 63, 1703–1726.
Chalmers, H., Gibbins, J., 2007. Initial evaluation of the impact of post-combustion capture of carbon dioxide on supercritical pulverised coal power plant part load performance. Fuel 86, 2109–2123.
Chalmers, H., Lucquiaud, M., Gibbins, J., Leach, M., 2009. Flexible operation of coal fired power plants with postcombustion capture of carbon dioxide. J. Environ. Eng. 135, 449–458.
Committee on Climate Change, 2013. 4th Carbon Budget Review Part 2 [.pdf], Available at: https://www.theccc.org.uk/publication/fourth-carbon-budget-review/ (accessed October 2015).
van Eckeveld, A.C., van der Ham, L.V., Geers, L.F.G., van den Broeke, L.J.P., Boersma, B.J., Goetheer, E.L.V., 2014. Online monitoring of the solvent and absorbed acid gas concentration in a CO_2 capture process using monoethanolamine. Ind. Eng. Chem. Res. 53, 5515–5523.
Eisfeld, T., Feldmüller, A., 2013. Fast cycling and fast start capability of combined cycle power plants with SGT5-4000F gas turbines. In: IMechE Seminar: Demand Response and Flexible Operation in UK Power Stations, 28 November, Nottingham, p. 2013.
Energy Technologies Institute, 2015. Building the UK Carbon Capture and Storage Sector – Scenarios and Actions [.pdf], Available at: http://www.eti.co.uk/wp-content/uploads/2015/03/CCS-Building-the-UK-carbon-capture-and-storage-sector-by-2013.pdf (accessed November 2015).
Faber, R., Köpcke, M., Biede, O., Knudsen, J.N., Andersen, J., 2011. Open-loop step responses for the MEA post-combustion capture process: experimental results from the Esbjerg pilot plant. Energy Procedia 4, 1427–1434.
Fitzgerald, F.D., Hume, S.A., McGough, G., Damen, K., 2014. Ferrybridge CCPilot100+ operating experience and final test results. Energy Procedia 63, 6239–6251.
Fløⁱ, N.E., Zangrilli, L., Mangiaracina, A., Mejdell, T., Kvamsdal, H.M., Hillestad, M., 2014. Validation of a dynamic model of the Brindisi pilot plant. Energy Procedia 63, 1040–1054.
Fløⁱ, N.E., Knuutila, H., Kvamsdal, H.M., Hillestad, M., 2015. Dynamic model validation of the post-combustion CO_2 absorption process. Int. J. Greenh. Gas Control 41, 127–141.
Global CCS Institute, 2014. The Global Status of CCS: 2014, Melbourne, Australia.
van der Ham, L.V., van Eckeveld, A.C., Goetheer, E.L.V., 2014. Online monitoring of dissolved CO_2 and MEA concentrations: effect of solvent degradation on predictive accuracy. Energy Procedia 63, 1223–1228.
Haines, M.R., Davison, J., 2014. Enhancing dynamic response of power plant with post-combustion capture using "Stripper stop". Int. J. Greenh. Gas Control 20, 49–56.
Hamborg, E.S., Smith, V., Cents, T., Brigman, N., Falk-Pedersen, O., De Cazenove, T., Chhaganlal, M., Feste, J.K., Ullestad, Ø., Ulvatn, H., Gorset, O., Askestad, I., Gram, L.K., Fostås, B.F., Shah, M.I., Maxson, A., Thimsen, D., 2014. Results from MEA testing at the CO_2 Technology Centre Mongstad, part II: verification of baseline results. Energy Procedia 63, 5994–6011.
IPCC, 2014. Climate Change 2014: Fifth Assessment Report of the Intergovernmental Panel on Climate Change. Cambridge University Press, Cambridge, UK.
Jordal, K., Ystad, P.A.M., Anantharaman, R., Chikukwa, A., Bolland, O., 2012. Design-point and part-load considerations for natural gas combined cycle plants with post combustion capture. Int. J. Greenh. Gas Control 11, 271–282.
Kvamsdal, H.M., Chikuwa, A., Hillestad, M., Zakeri, A., Einbu, A., 2011. A comparison of different parameter correlation models and the validation of an MEA-based absorber model. Energy Procedia 4, 1526–1533.
Lucquiaud, M., Fernandez, E.S., Chalmers, H., Mac Dowell, M., Gibbins, J., 2014. Enhanced operating flexibility and optimised off-design operation of coal plants with post-combustion capture. Energy Procedia 63, 7495–7507.
Mac Dowell, N., Shah, N., 2014. Optimisation of post-combustion CO_2 capture for flexible operation. Energy Procedia 63, 1525–1535.
Mechleri, E., 2015. Controllability analysis of a post-combustion CO_2 capture plant integrated with a coal and natural gas-fired power plan. In: 3rd Post Combustion Capture Conference, 9th September 2015, Regina, Canada.
Mejdell, T., Vassbotn, T., Juliussen, O., Tobiesen, A., Einbu, A., Knuutila, H., Hoff, K.A., Andersson, V., Svendsen, H., 2011. Novel full height pilot plant for solvent development and model validation. Energy Procedia 4, 1753–1760.
Murray, S., 2013. Why whole portfolio modelling is essential. In: IPA 5th Annual Conference, 12 March 2013, East Kilbride.
Oates, D.L., Versteeg, P., Hittinger, E., Jaramillo, P., 2014. Profitability of CCS with flue gas bypass and solvent storage. Int. J. Greenh. Gas Control 27, 279–288.
Pöyry, 2009. Impact of Intermittency, How Wind Variability Could Change the Shape of British and Irish Energy Markets [.pdf], Available at: www.poyry.co.uk/sites/www.poyry.uk/files/IntermittencyMethodologyv1_0.pdf (accessed March 2015).
Notz, R., Mangalapally, H.P., Hasse, H., 2012. Post combustion CO_2 capture by reactive absorption: pilot plant description and results of systematic studies with MEA. Int. J. Greenh. Gas Control 6, 84–112.
Rabensteiner, M., Kinger, G., Koller, M., Gronald, G., Hochenhauer, C., 2014. Pilot plant study of ethylenediamine as a solvent for post combustion carbon dioxide capture and comparison to monoethanolamine. Int. J. Greenh. Gas Control 27, 1–14.
Seibert, F., Chen, E., Perry, M., Briggs, S., Montgomery, R., Rochelle, G., 2011. UT/SRP CO_2 capture pilot plant – operating experience and procedures. Energy Procedia 4, 1616–1623.
Ystad, M.P.A., Bolland, O., Hillestad, M., 2012. NGCC and hard-coal power plant with CO_2 capture based on absorption. Energy Procedia 23, 33–44.

Please cite this article in press as: Tait, P., et al., A pilot-scale study of dynamic response scenarios for the flexible operation of post-combustion CO_2 capture. Int. J. Greenhouse Gas Control (2015), http://dx.doi.org/10.1016/j.ijggc.2015.12.009